Electronic Supplementary Material (ESI) for Journal of Materials Chemistry A

Contents

1 Rationale for the systems with 2 Al atoms or 1 Al and one defect

The placement of Al atoms and defects to generate the different systems investigated obeyed the following rationale: for the BB and BP series, the position of one bridging Al is always the same ($B_{2,5}$), and the different positions of the second bridging Al or of the pairing Al give rise to different configurations. Similarly for the DB and DP series, where the position of the defect was always similar (and corresponded to the position of the fixed Al in the BB and BP series, $D_{2,5}$). For the PP series the position of one pairing Al is common to all systems ($P_{2,6}$), and the one of the second Al is varied. One then generates all possible configurations for our calculation cell (note the use of periodic boundary conditions), subject to two restrictions:

- from symmetry equivalent configurations only one is kept. As an example, this makes it unnecessary in some cases to generate structures where the second modification is done in a dreierketten chain to the left of the first one, rather than to the right (in the sense of viewing as in Figure 1). The symmetry considered is that of the upper leaflet of the base tobermorite crystal structure (no H's; see also the "Details of the geometry optimization strategy" section below for an exact definition of the upper leaflet)

- for some series one further imposes a distance cutoff; systems with bigger Al-Al (or Defect-Al) distances are not considered. In particular:

  - a 12 Å cutoff was used for the $P_{2,6}P_{3,i}$ sub-series
  - a 13 Å cutoff was used for the $B_{2,5}P_{3,i}$; $B_{2,5}P_{1,i}$; $B_{2,5}P_{4,i}$; $D_{2,5}P_{3,i}$; $D_{2,5}P_{1,i}$ and $D_{2,5}P_{4,i}$ sub-series
  - a 15 Å cutoff was used for the $B_{2,5}B_{4,i}$ and $D_{2,5}B_{4,i}$ sub-series

where in all cases i represents a generic tetrahedron position in the given dreierketten chain. The sub-series mentioned just above basically correspond to subgroups of systems

where the second modification is done in the next-neighbour or next-next-neighbour chain as compared to the first one. The cutoffs have no special meaning, they are merely conditions which the studied systems happen to obey. Furthermore, for the $P_{2,6}P_{4,i}$ sub-series it is perhaps more informative to say simply that two configurations were generated (see below). As can be better appreciated from the discussion in the body of the paper, whole this procedure gave rise to more than enough systems to support our conclusions.

2 Molecular representations of the systems in Figure 2

2.1 General introductory notes on the molecular representations in this file

In the molecular representations of the systems in Supp. Figures 1 to 57, 59, 60 and 62 to 65 the last step of the UPPERLEAFLET geometry optimization is shown (more details below). All the structures are also provided in .xyz format. A different molecular representation was chosen compared to the one used in Figure 1. This is intended to give a "quick preview" of each structure for the reader wishing to check some detail without having to go as far as plotting the corresponding .xyz file. The same color coding as before is used: grey for Ca, yellow for Si, red for O, white for H and blue for Al. It was not deemed necessary to (laboriously) edit out the obviously non-existing Ca-Ca bonds which are automatically produced by the visulaization program employed. Note that in this representation, unlike in Figure 1, atoms both in the upper and lower leaflets of the structure are seen (more details below). Note also that the current representation corresponds to a visualization of exactly the supercell used in the calculations, with 608 atoms.

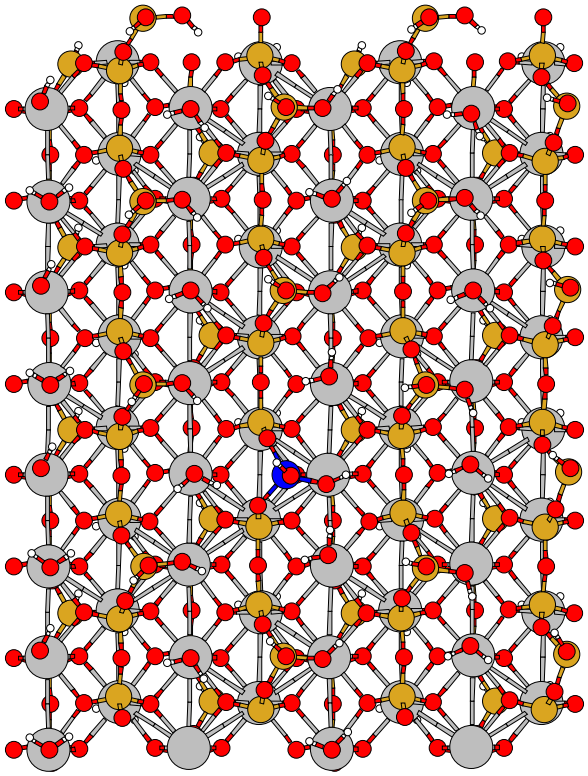

Supp. Figure 1: The BRIDGE structure.

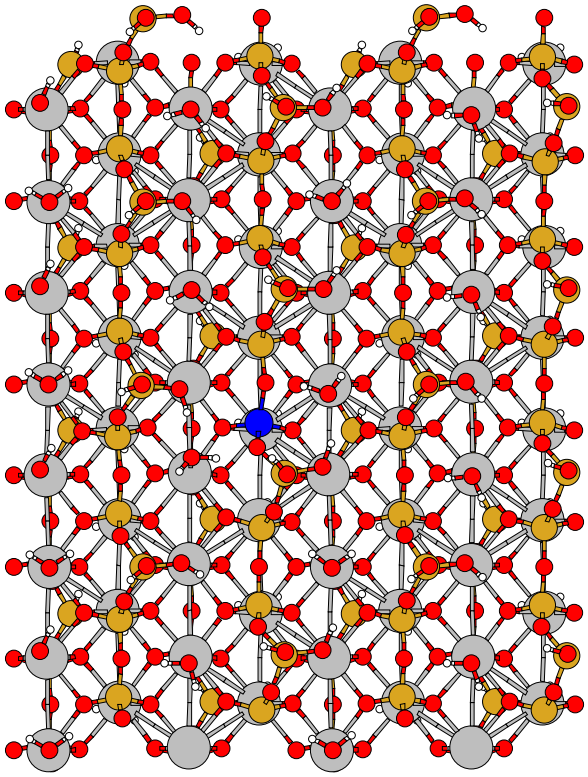

Supp. Figure 2: The PAIR structure.

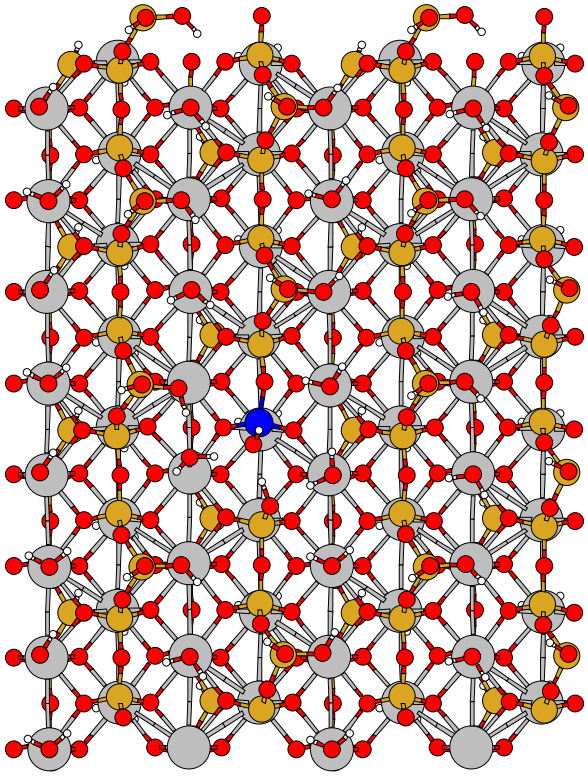

Supp. Figure 3: The EOC structure ($D_{2,5}P_{2,6}$ in the systematic naming used below for the BB, BP, PP, DB and DP series).

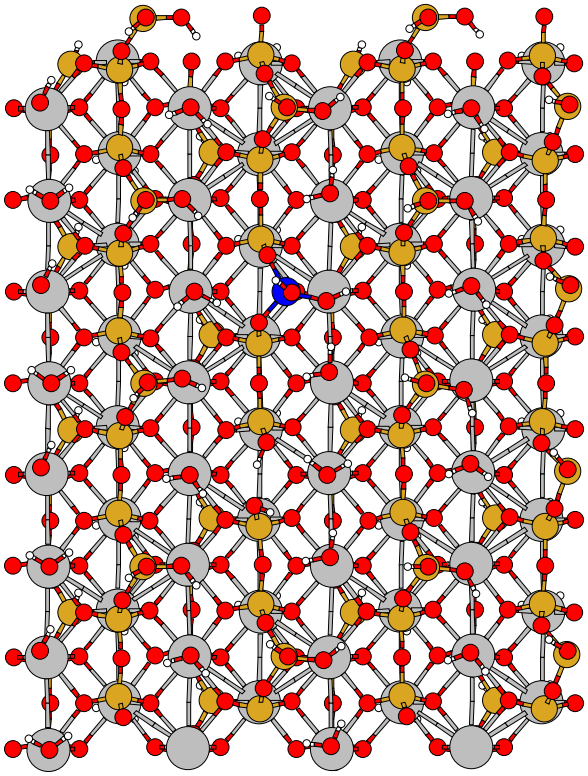

Supp. Figure 4: The EOC_ref ($D_{2,5}B_{2,8}$) structure.

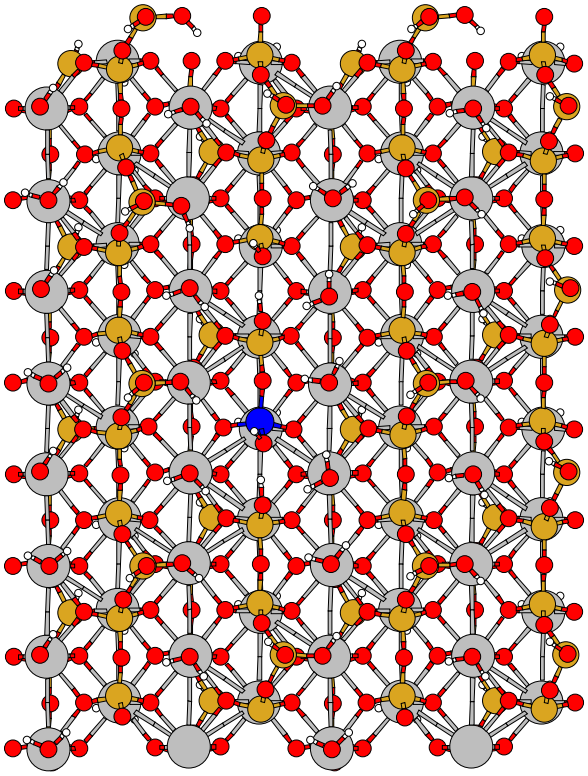

Supp. Figure 5: The DIMER structure.

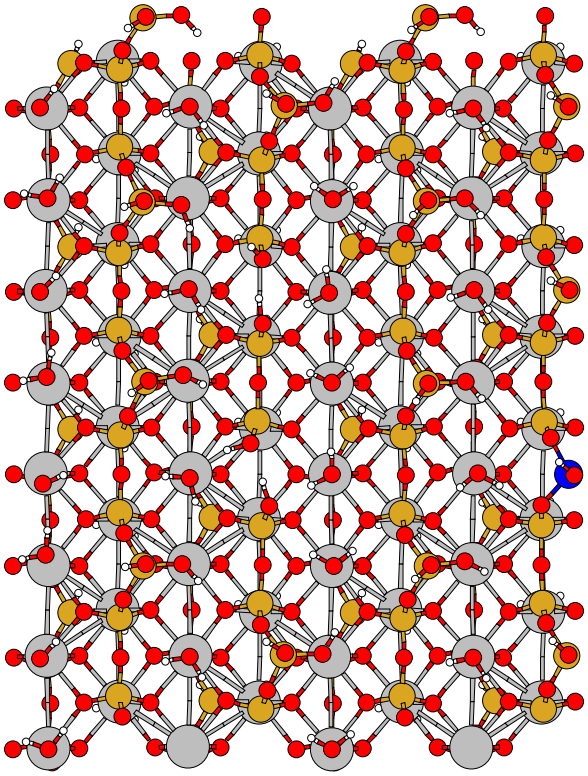

Supp. Figure 6: The DIMER_ref structure.

3 Molecular representations of the systems for Figure 3

3.1 Two Al in Bridging positions (BB)

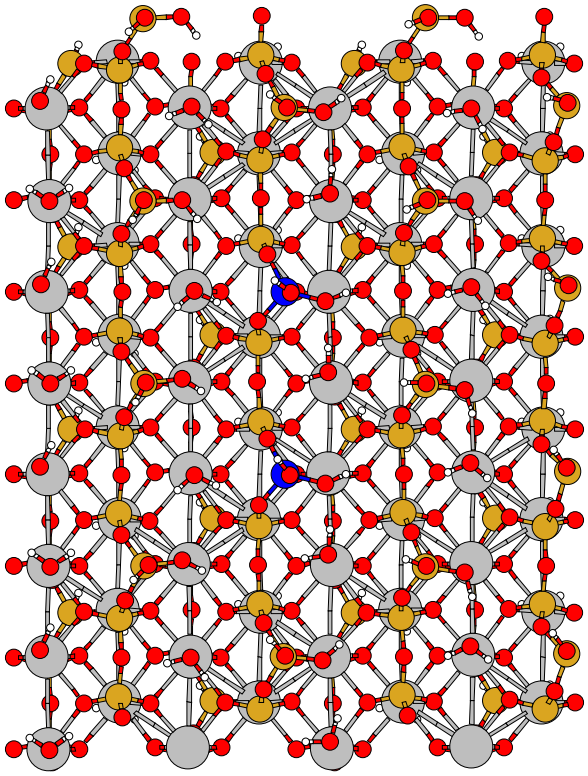

Supp. Figure 7: The $B_{2,5}B_{2,8}$ structure.

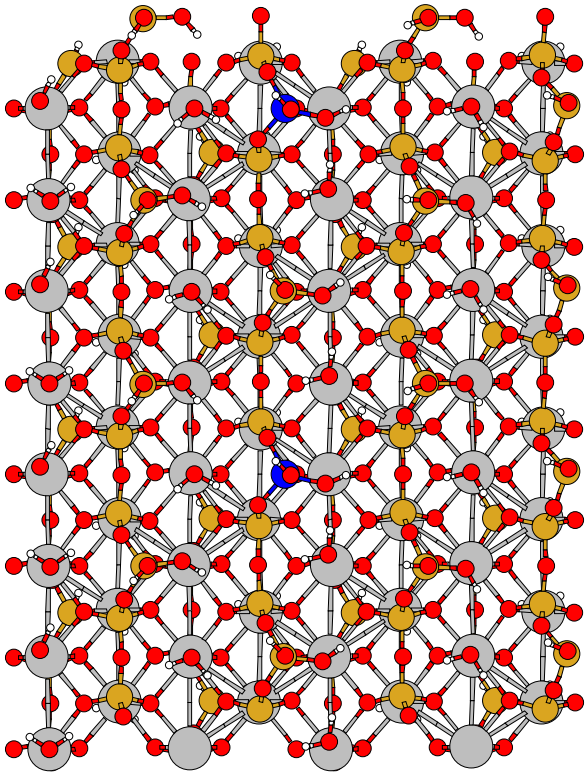

Supp. Figure 8: The $B_{2,5}B_{2,11}$ structure.

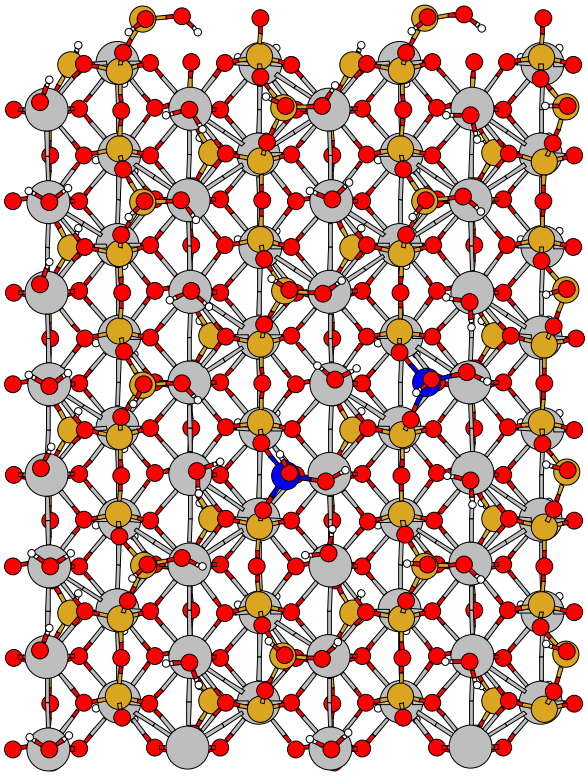

Supp. Figure 9: The $B_{2,5}B_{3,6}$ structure.

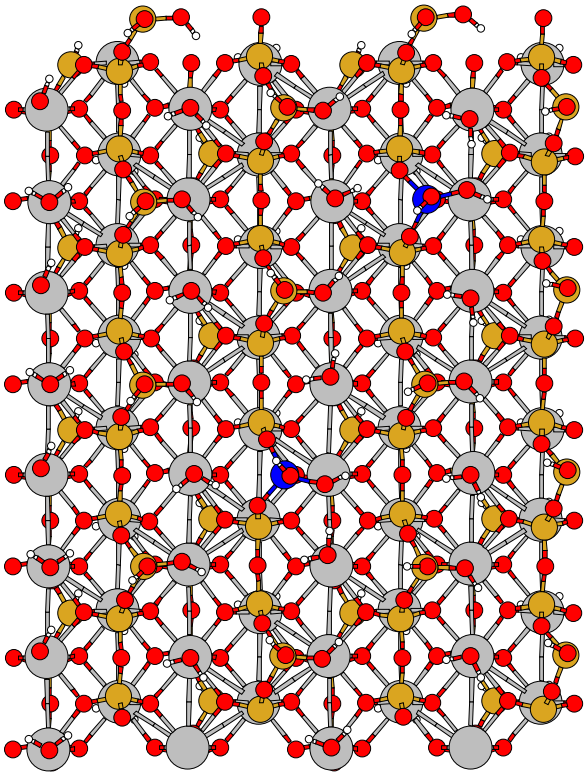

Supp. Figure 10: The $B_{2,5}B_{3,9}$ structure.

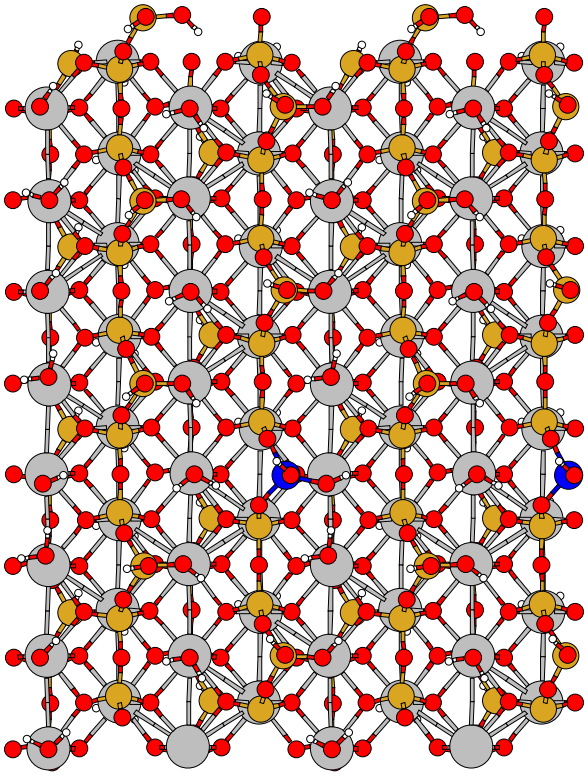

Supp. Figure 11: The $B_{2,5}B_{4,5}$ structure.

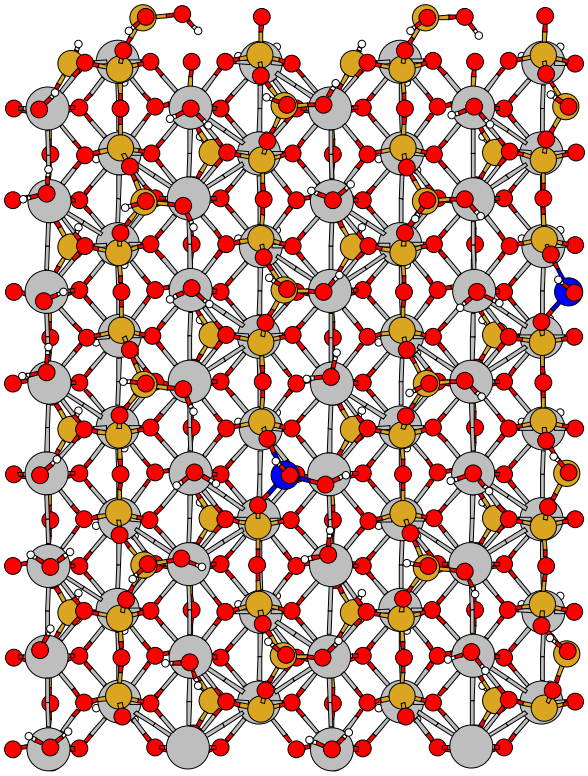

Supp. Figure 12: The $B_{2,5}B_{4,8}$ structure.

3.2 One Al in a Bridging position and one Al in a Pairing position (BP)

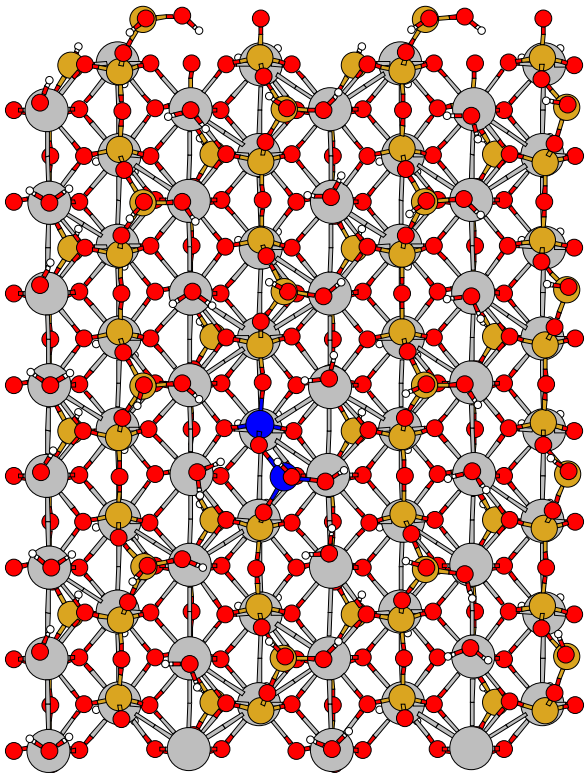

Supp. Figure 13: The $B_{2,5}P_{2,6}$ structure.

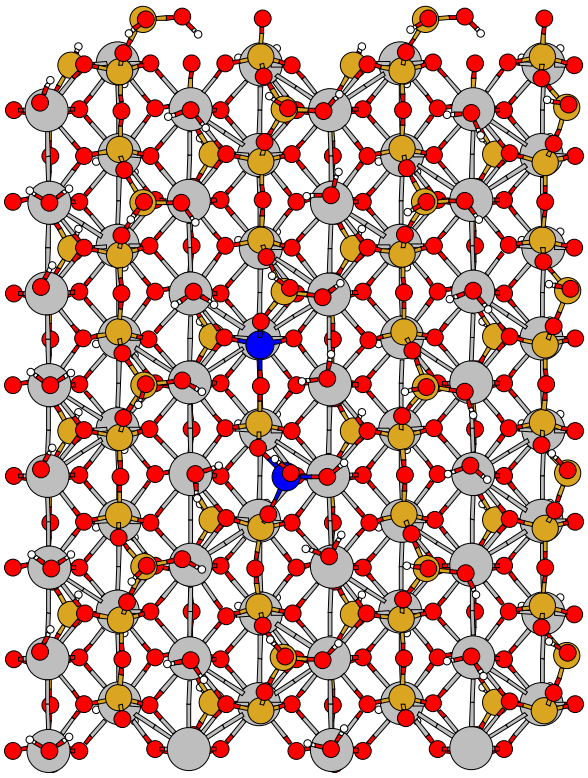

Supp. Figure 14: The $B_{2,5}P_{2,7}$ structure.

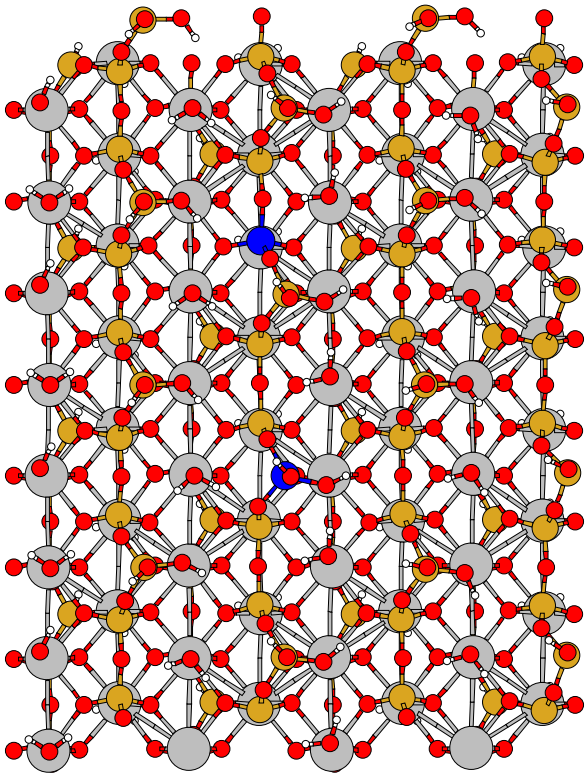

Supp. Figure 15: The $B_{2,5}P_{2,9}$ structure.

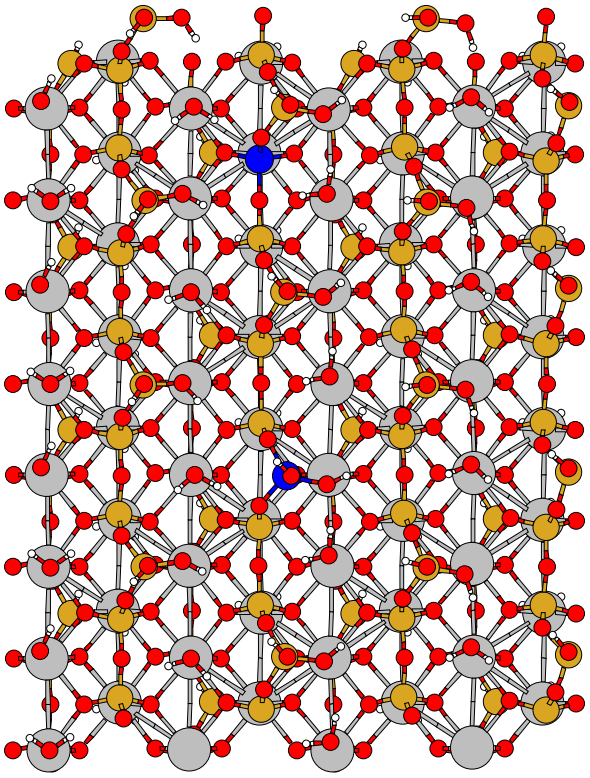

Supp. Figure 16: The $B_{2,5}P_{2,10}$ structure.

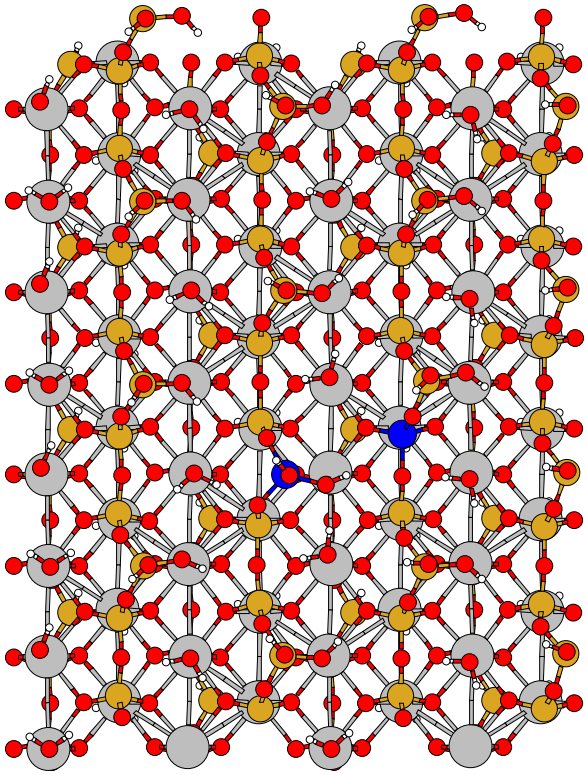

Supp. Figure 17: The $B_{2,5}P_{3,5}$ structure.

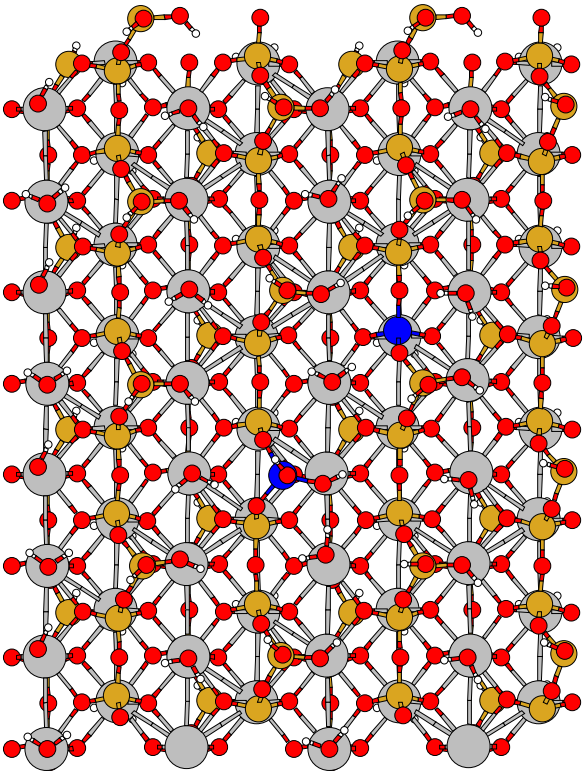

Supp. Figure 18: The $B_{2,5}P_{3,7}$ structure.

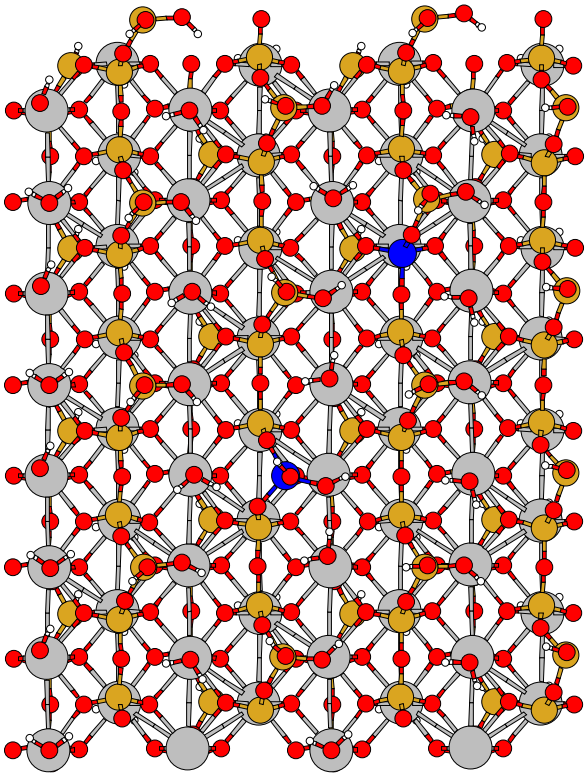

Supp. Figure 19: The $B_{2,5}P_{3,8}$ structure.

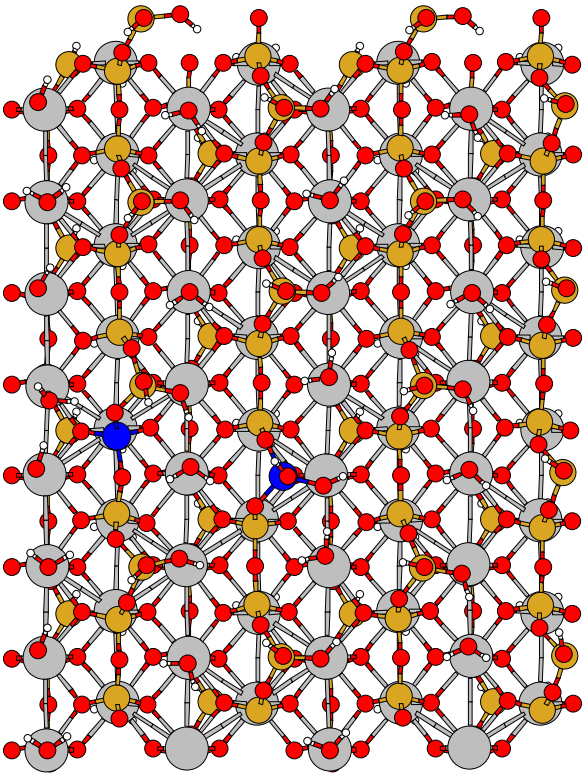

Supp. Figure 20: The $B_{2,5}P_{1,5}$ structure.

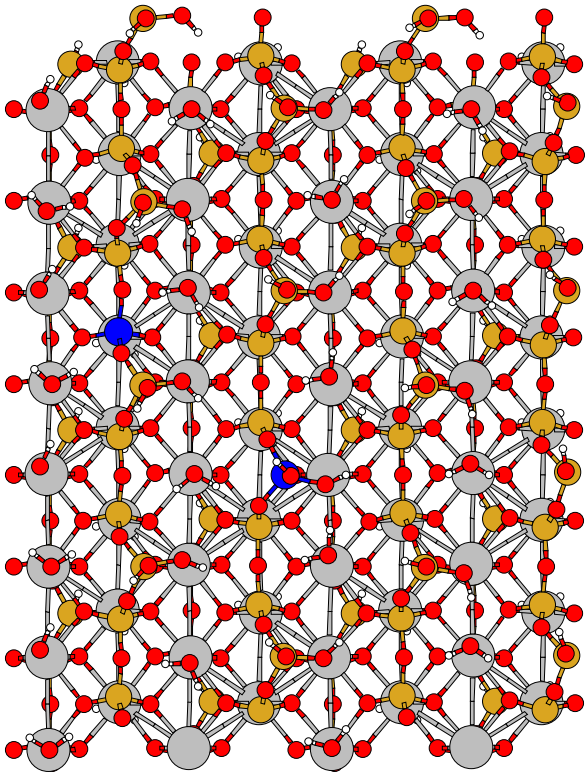

Supp. Figure 21: The $B_{2,5}P_{1,7}$ structure.

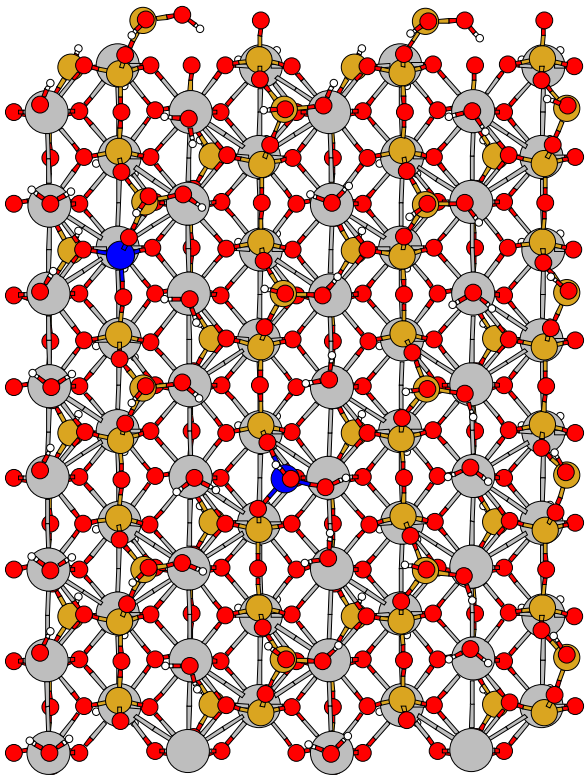

Supp. Figure 22: The $B_{2,5}P_{1,8}$ structure.

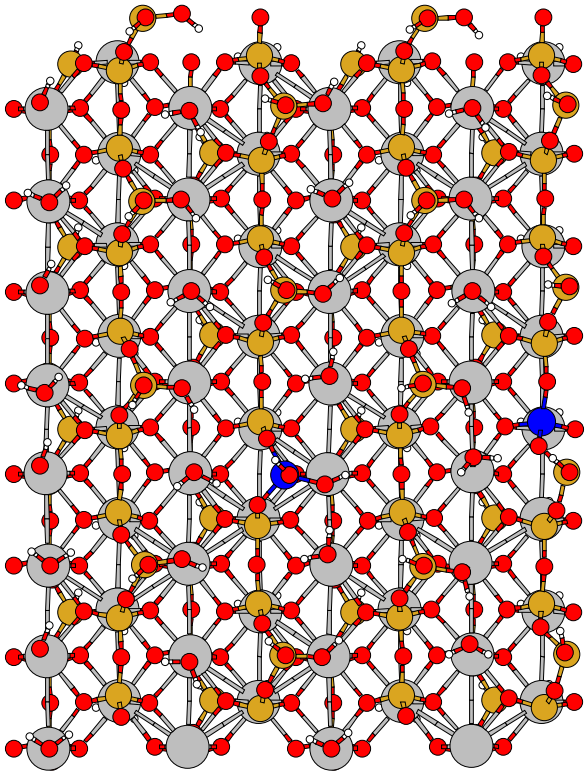

Supp. Figure 23: The $B_{2,5}P_{4,6}$ structure.

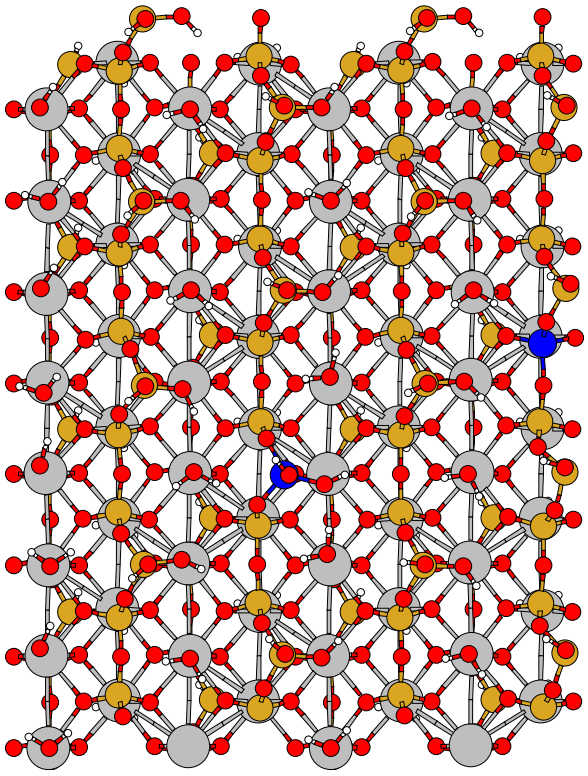

Supp. Figure 24: The $B_{2,5}P_{4,7}$ structure.

3.3 Two Al in Pairing positions (PP)

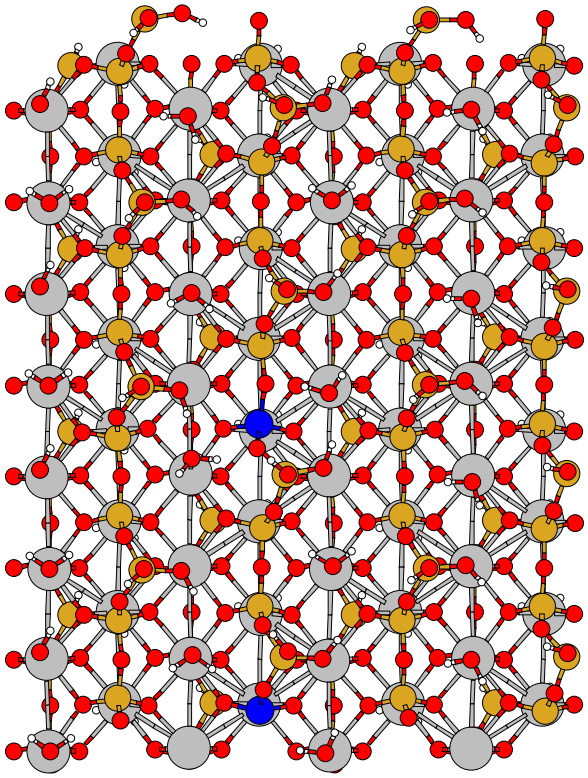

Supp. Figure 25: The $P_{2,6}P_{2,1}$ structure.

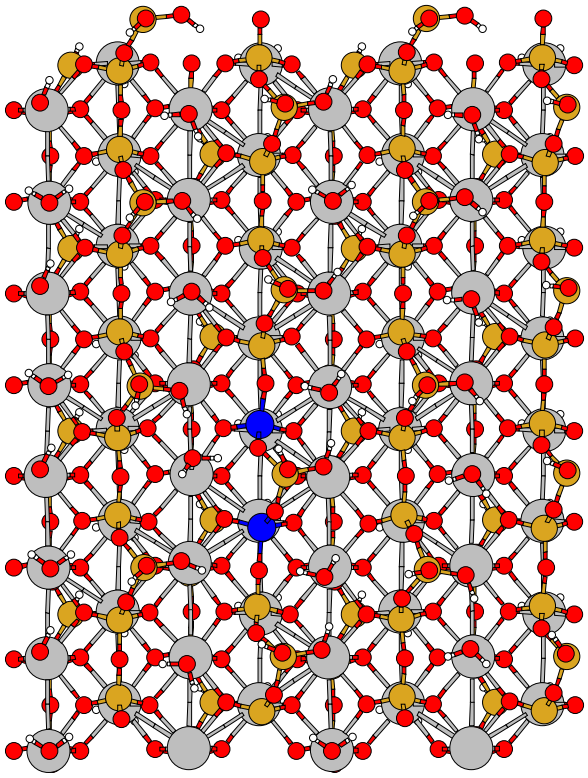

Supp. Figure 26: The $P_{2,6}P_{2,4}$ structure.

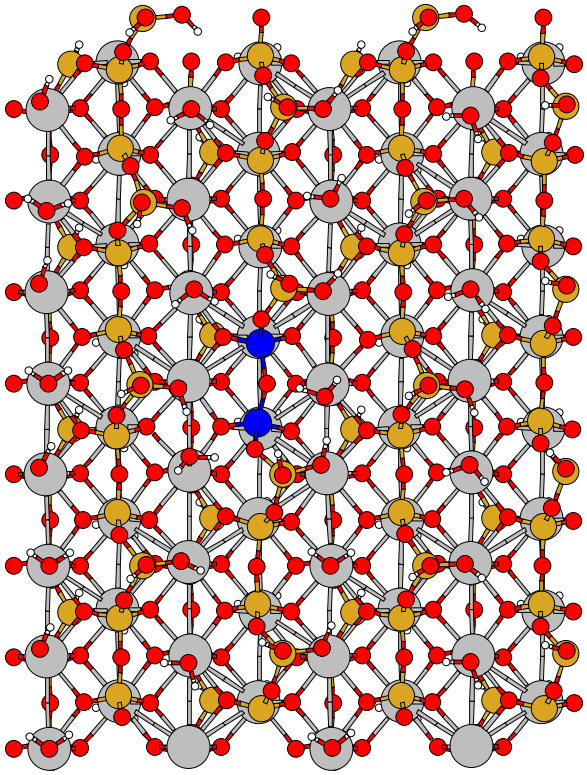

Supp. Figure 27: The $P_{2,6}P_{2,7}$ structure.

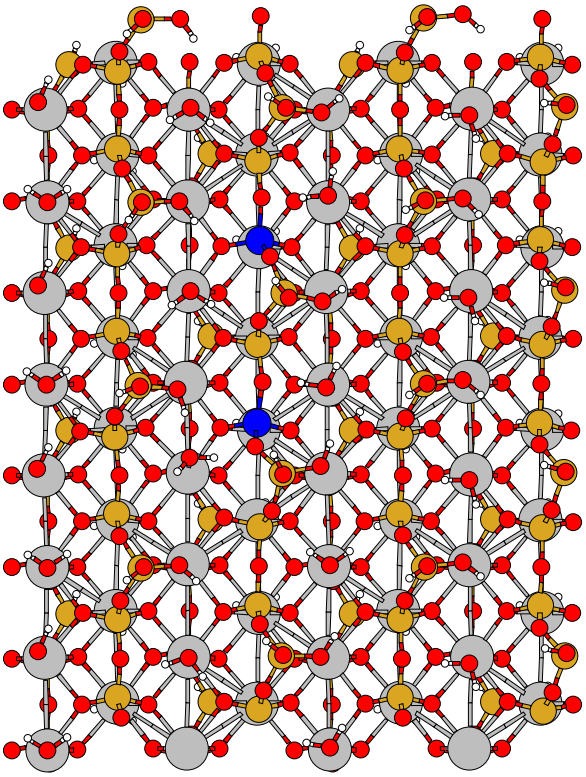

Supp. Figure 28: The $P_{2,6}P_{2,9}$ structure.

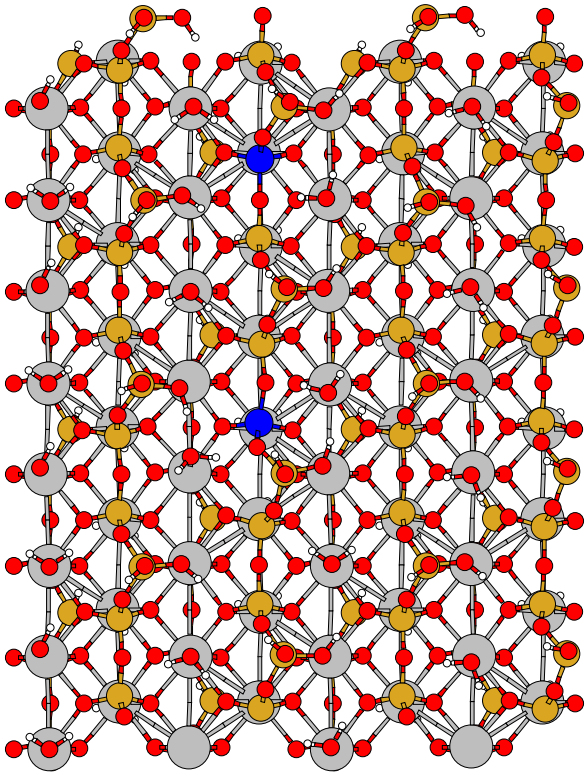

Supp. Figure 29: The $P_{2,6}P_{2,10}$ structure.

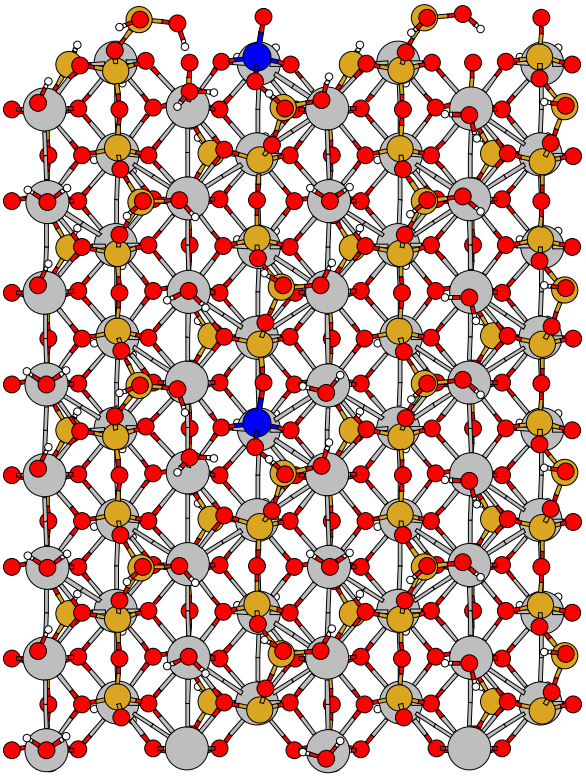

Supp. Figure 30: The $P_{2,6}P_{2,12}$ structure.

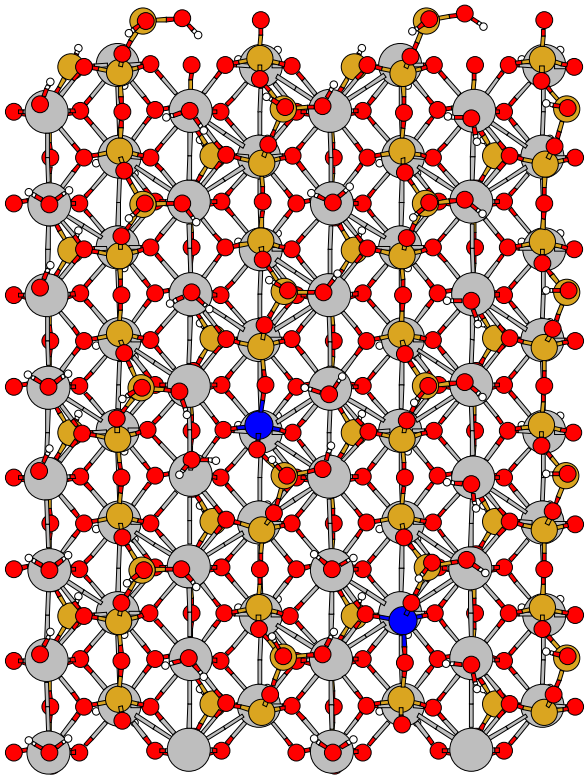

Supp. Figure 31: The $P_{2,6}P_{3,2}$ structure.

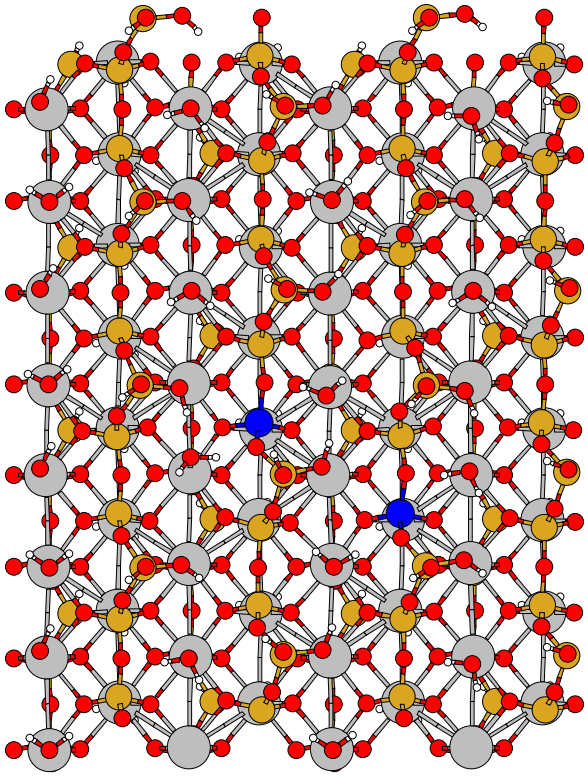

Supp. Figure 32: The $P_{2,6}P_{3,4}$ structure.

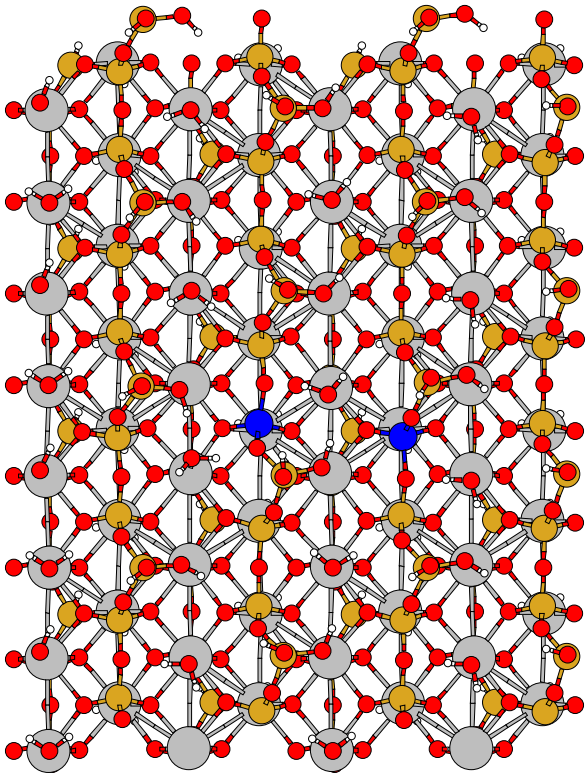

Supp. Figure 33: The $P_{2,6}P_{3,5}$ structure.

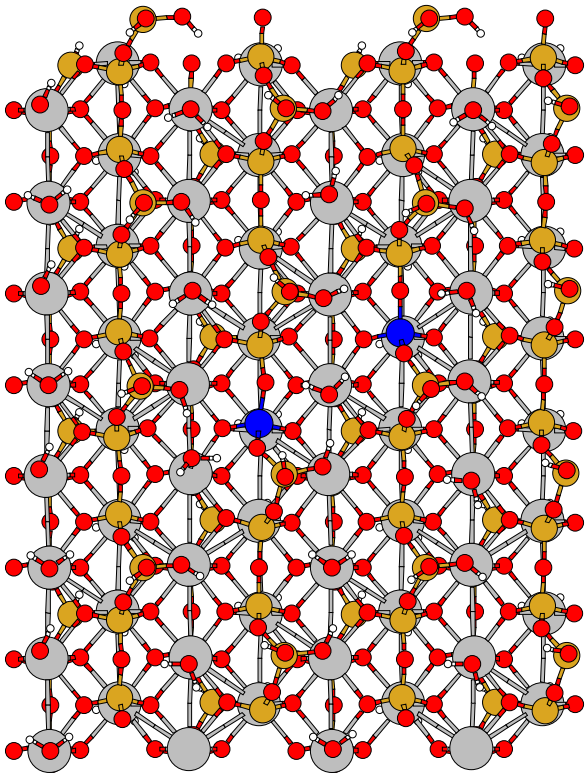

Supp. Figure 34: The $P_{2,6}P_{3,7}$ structure.

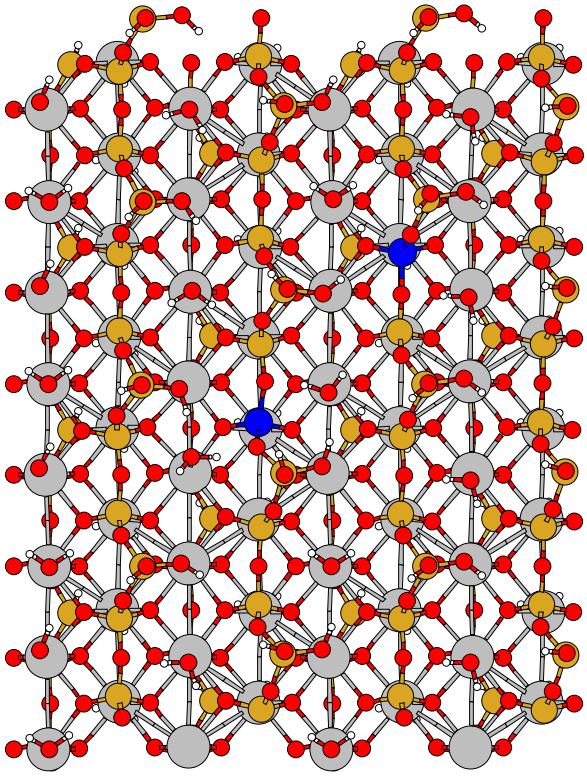

Supp. Figure 35: The $P_{2,6}P_{3,8}$ structure.

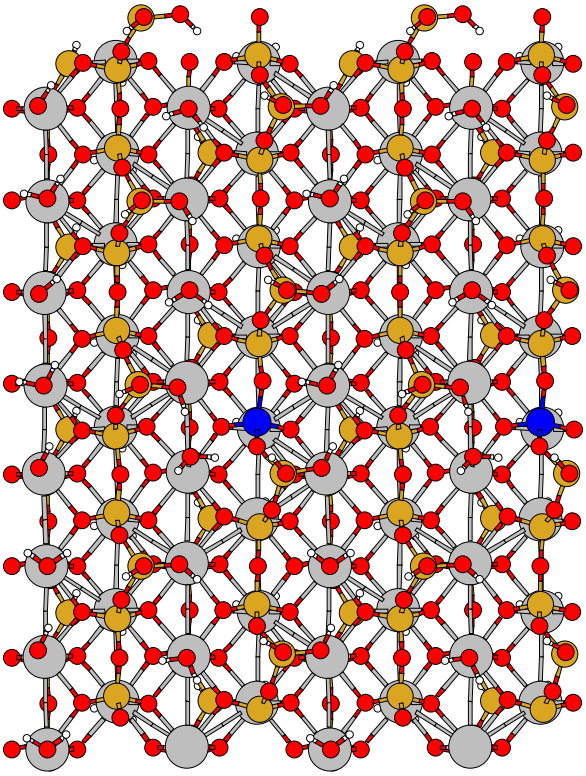

Supp. Figure 36: The $P_{2,6}P_{4,6}$ structure.

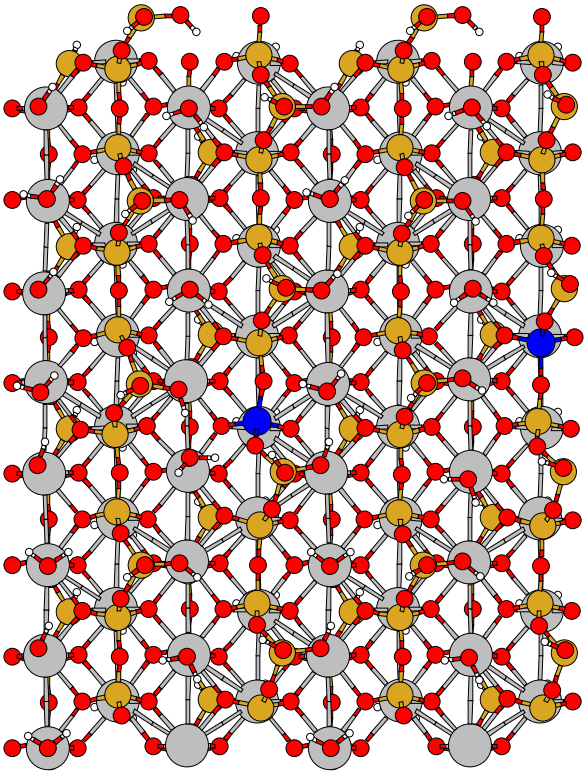

Supp. Figure 37: The $P_{2,6}P_{4,7}$ structure.

4 Molecular representations of the systems for Figure 4

Note that the location of the defect (D) is always the same and as in Figure 1.

4.1 One Defect and one Al in a Bridging position (DB)

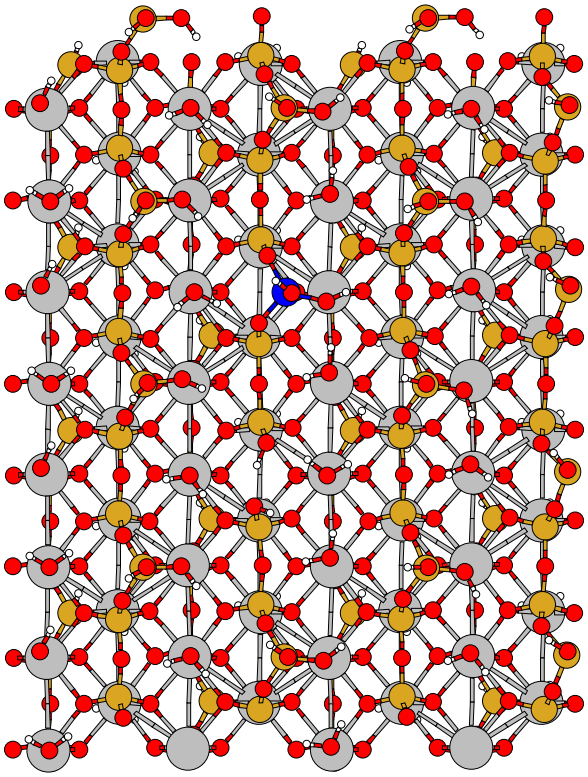

Supp. Figure 38: The $D_{2,5}B_{2,8}$ structure.

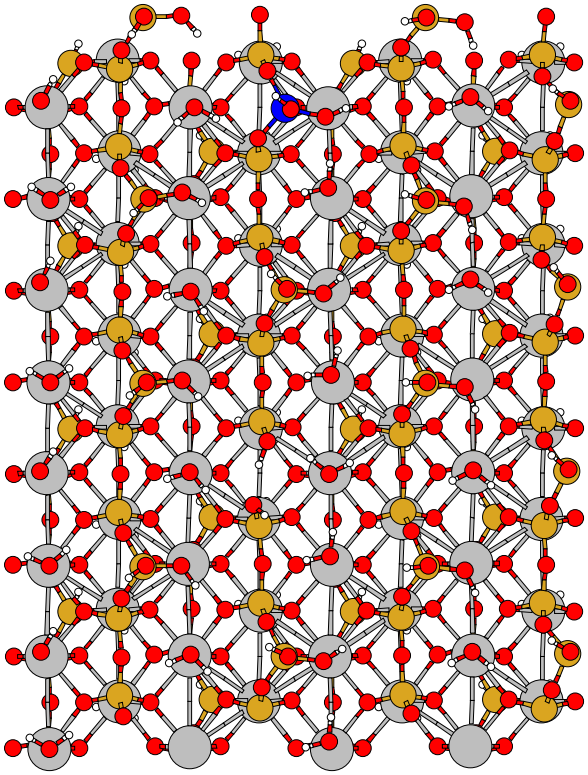

Supp. Figure 39: The $D_{2,5}B_{2,11}$ structure.

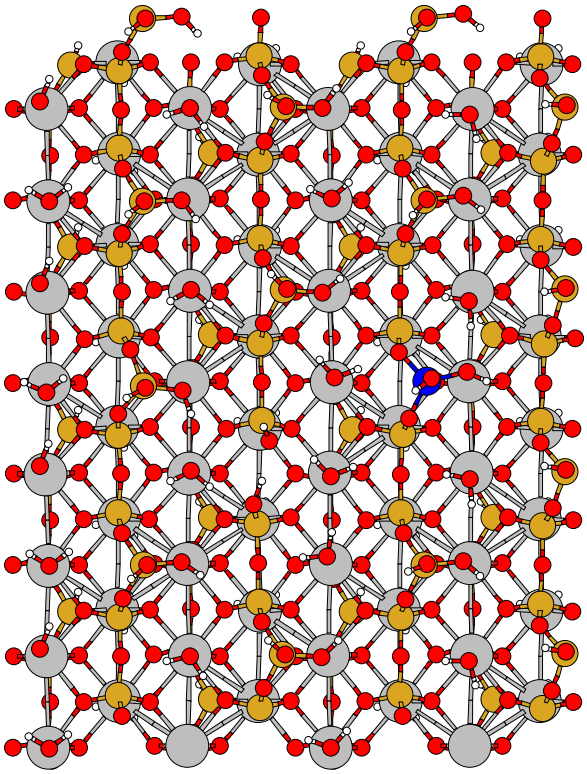

Supp. Figure 40: The $D_{2,5}B_{3,6}$ structure.

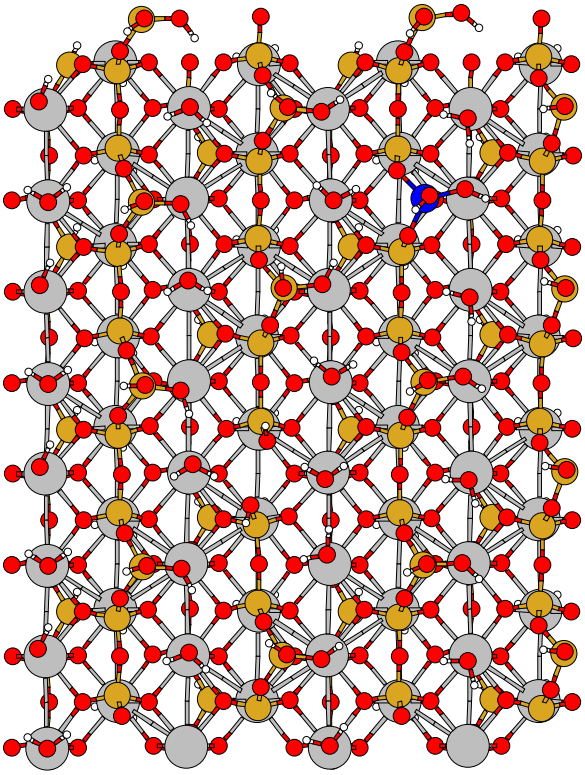

Supp. Figure 41: The $D_{2,5}B_{3,9}$ structure.

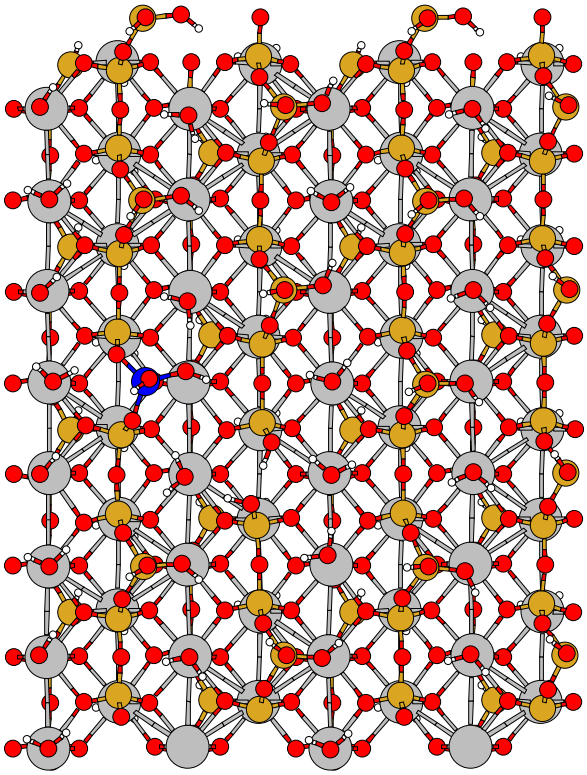

Supp. Figure 42: The $D_{2,5}B_{1,6}$ structure.

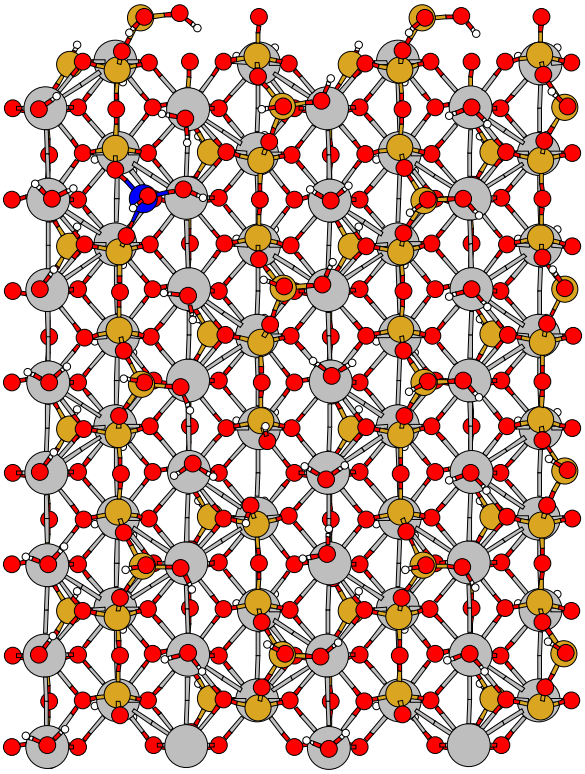

Supp. Figure 43: The $D_{2,5}B_{1,9}$ structure.

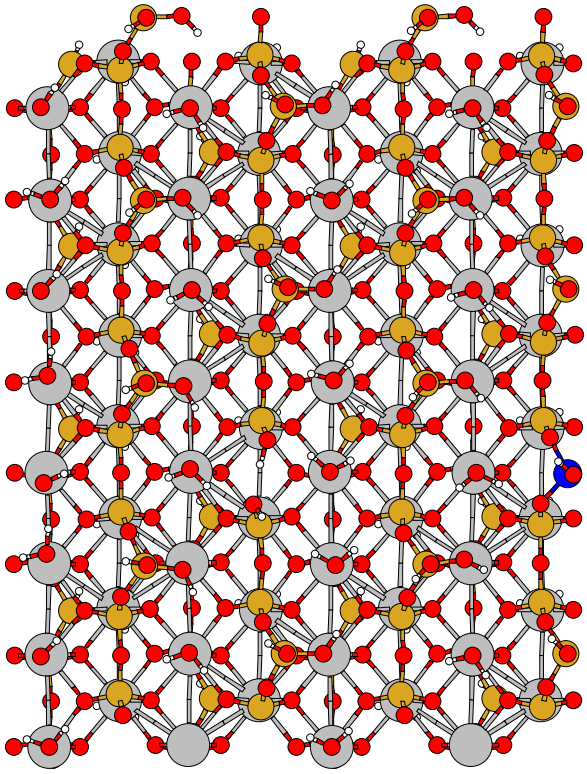

Supp. Figure 44: The $D_{2,5}B_{4,5}$ structure.

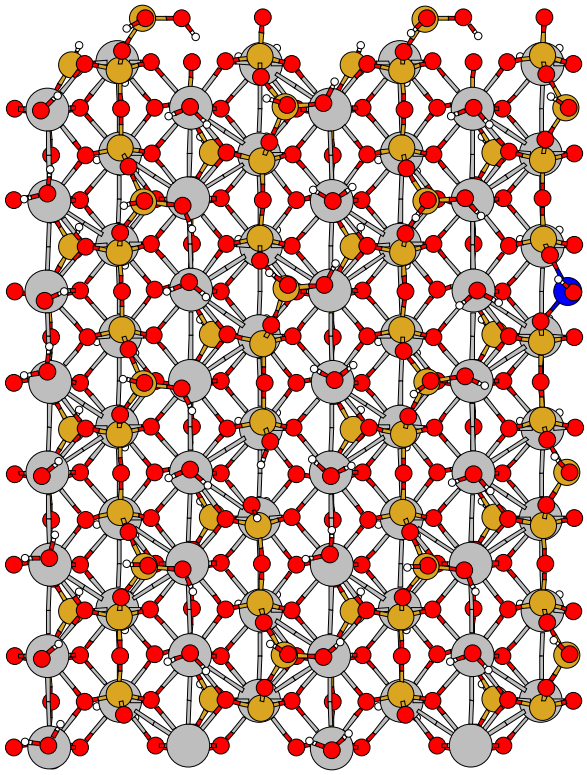

Supp. Figure 45: The $D_{2,5}B_{4,8}$ structure.

4.2 One Defect and one Al in a Pairing position (DP)

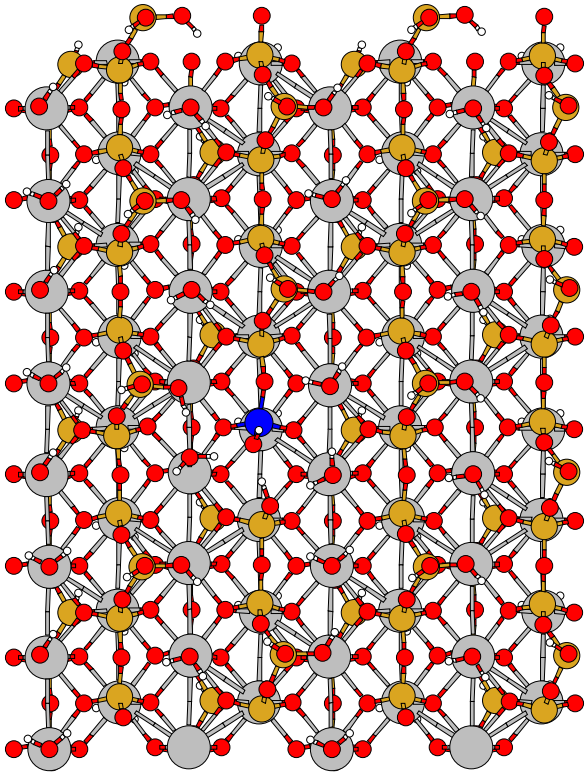

Supp. Figure 46: The $D_{2,5}P_{2,6}$ structure.

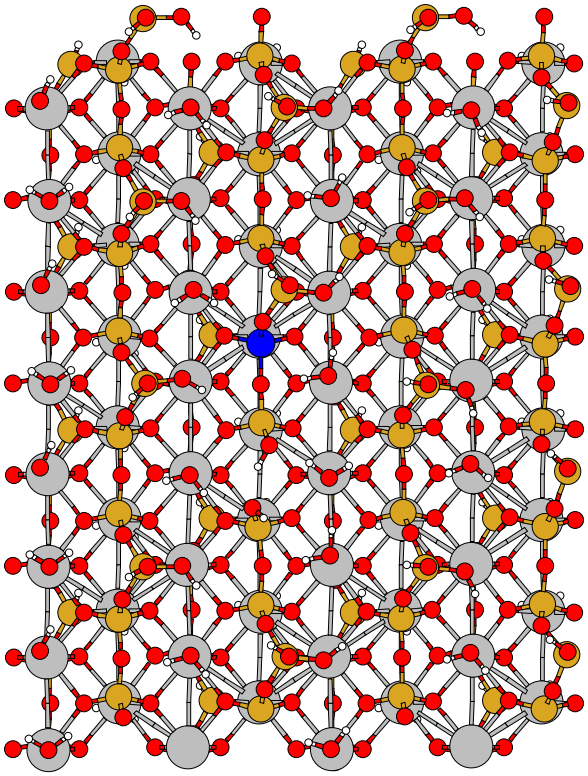

Supp. Figure 47: The $D_{2,5}P_{2,7}$ structure.

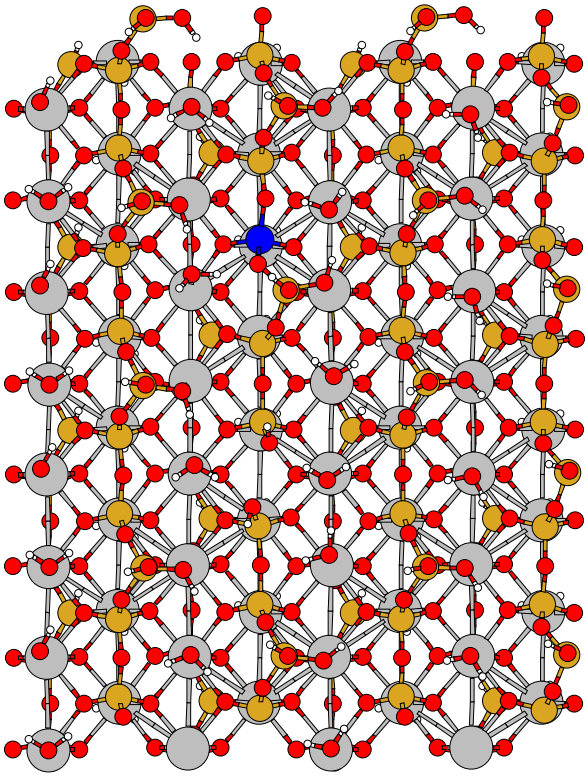

Supp. Figure 48: The $D_{2,5}P_{2,9}$ structure.

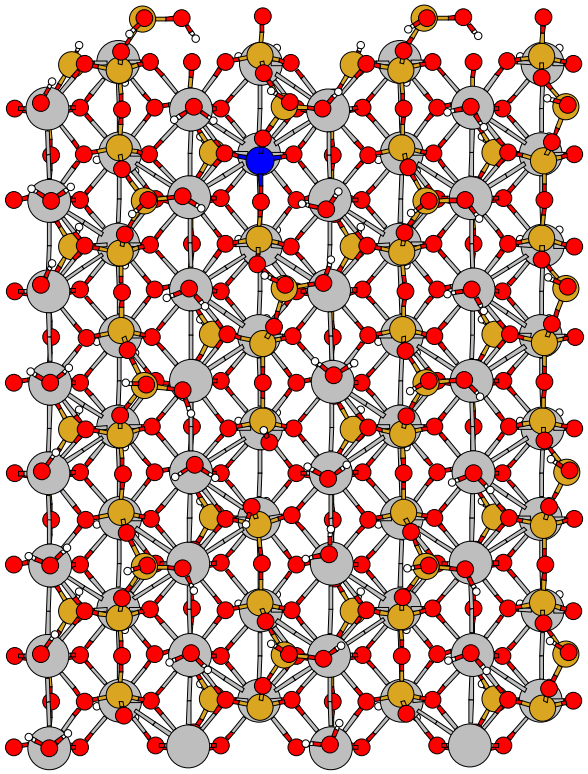

Supp. Figure 49: The $D_{2,5}P_{2,10}$ structure.

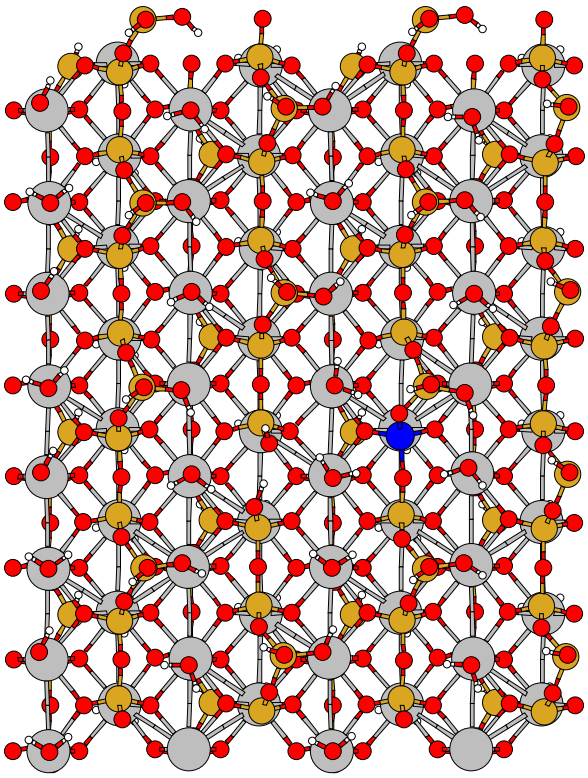

Supp. Figure 50: The $D_{2,5}P_{3,5}$ structure.

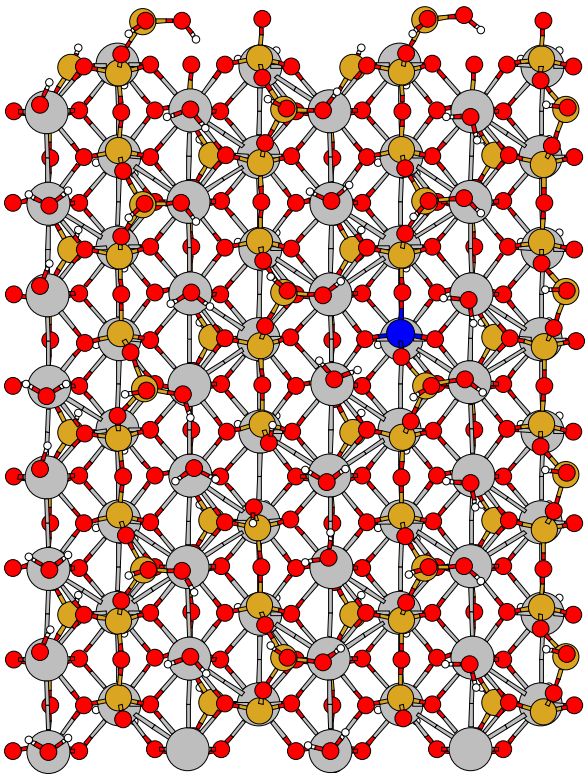

Supp. Figure 51: The $D_{2,5}P_{3,7}$ structure.

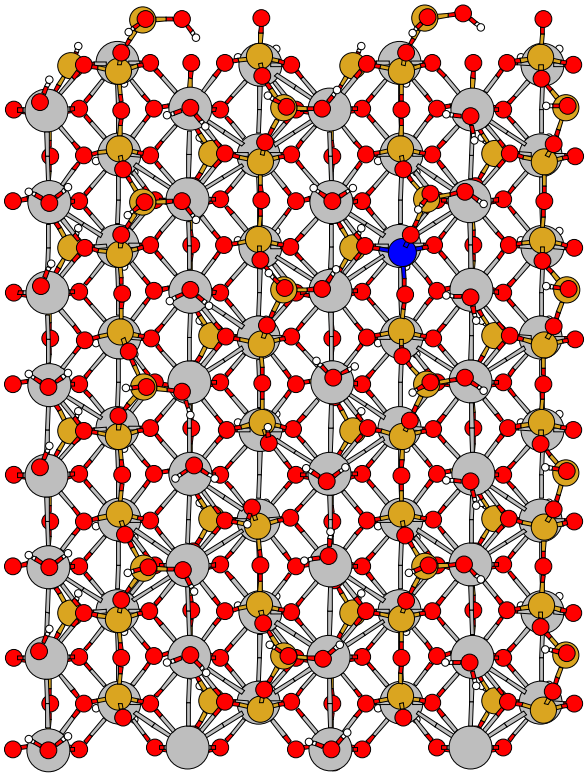

Supp. Figure 52: The $D_{2,5}P_{3,8}$ structure.

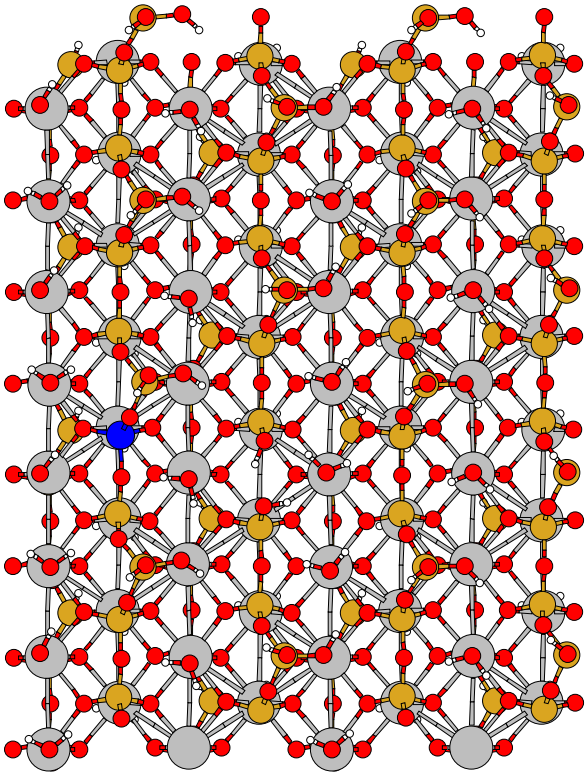

Supp. Figure 53: The $D_{2,5}P_{1,5}$ structure.

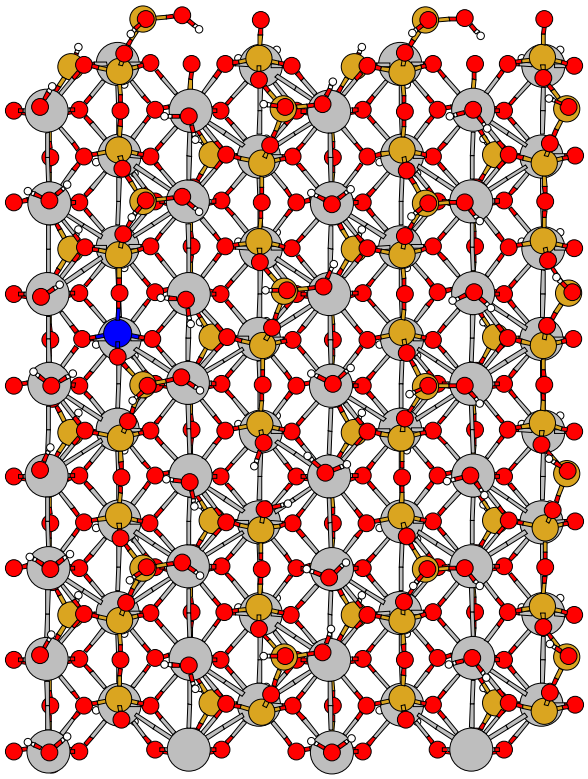

Supp. Figure 54: The $D_{2,5}P_{1,7}$ structure.

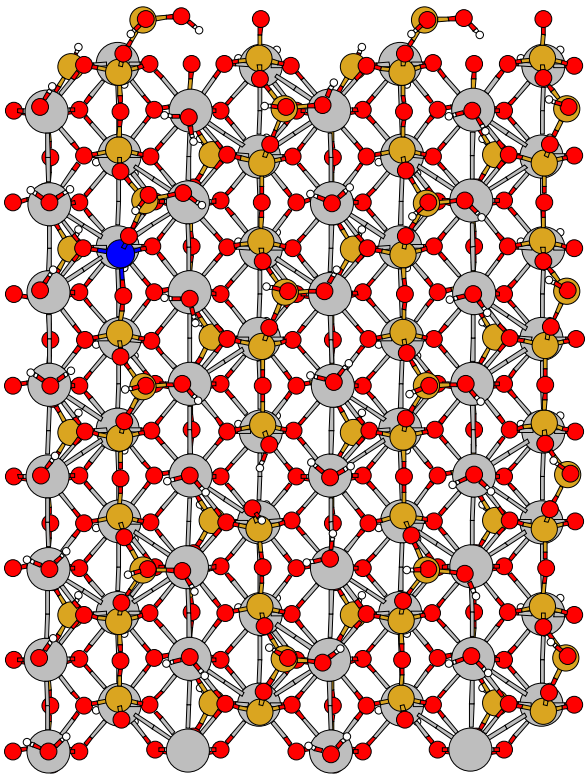

Supp. Figure 55: The $D_{2,5}P_{1,8}$ structure.

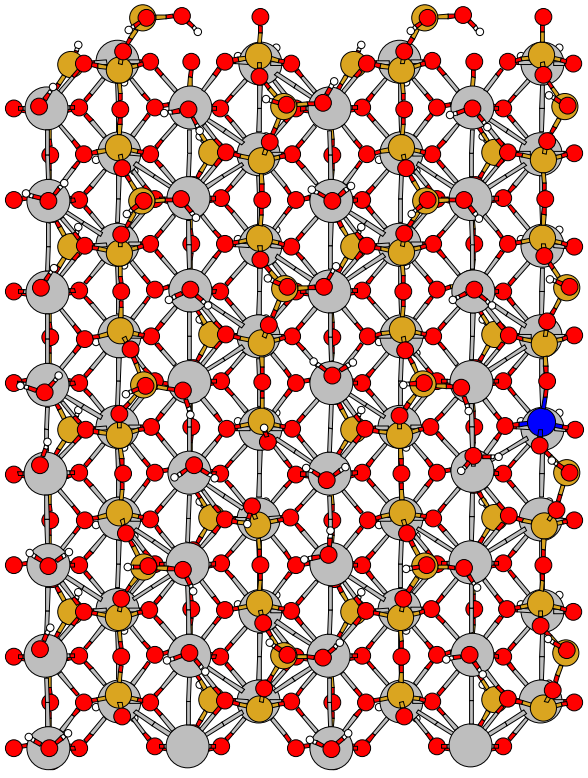

Supp. Figure 56: The $D_{2,5}P_{4,6}$ structure.

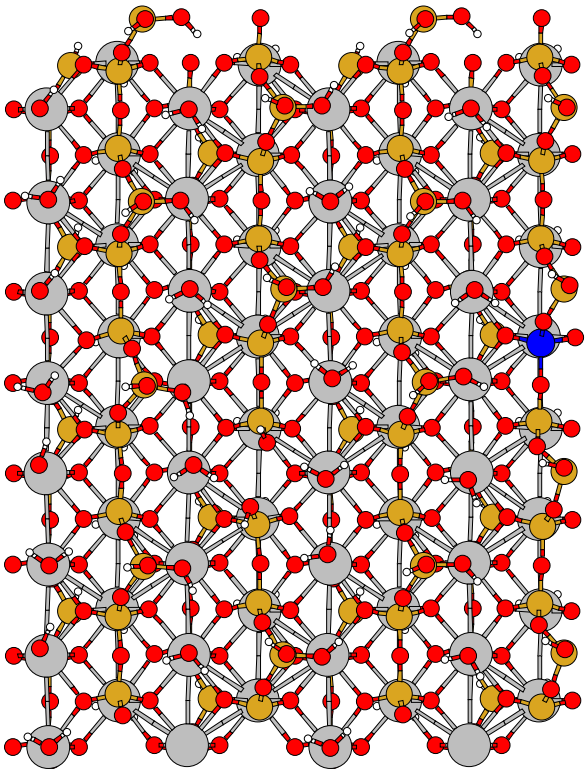

Supp. Figure 57: The $D_{2,5}P_{4,7}$ structure.

5 Details of the geometry optimization strategy

First of all a two-step geometry optimization of the unmodified C-S-H plate (essentially, what is displayed in Figure 1 but without the Al substitution and the defect, i.e., unmodified and infinite silicate dreierketten chains) was carried out, departing from the crystal structure of tobermorite. The added protons were initially placed perpendicular to the plate's surface (along the "z direction"), 1 Å from an O atom, in the case of the two O atoms which are only coordinated to one Si atom on every bridging tetrahedron, making two -OH groups. Furthermore, two H atoms were placed per O surface atom which is only coordinated to one Ca atom, making a water molecule, initially with a 180° H-O-H angle, 1 Å O-H bonds and placed along the cell "b" parameter. In the first step only the positions of the H atoms were optimized, followed by a full structural optimization. This structure was then used as the starting point for all other calculations.

The geometry optimizations for the systems containing Al substitutions and defects also followed a two-step procedure. The desired modifications are done in the above-described optimized plate, then one optimizes the "core region" around these modifications (JUST-CORE optimization), followed by an optimization of the upper half of the structure (where the changes are made, UPPERLEAFLET optimization). The core region consists of:

- in the case of Al substitutions in bridging tetrahedra, BT, of the Al atom itself plus the two connected -OH groups;
- in the case of Al substitutions in pairing tetrahedra, PT, of the Al atom itself plus the two O atoms which connect it to the two neighbouring Si atoms;
- whenever a defect is created, one removes a Si atom and an -OH group. One then needs to insert one proton on each of the O atoms in two different PT which previously were connected to the removed BT. One also needs to "transform" what was previously the second -OH group from the removed BT, coordinating to a Ca atom, into a water molecule by adding a proton. The initial configurations for these 4 protons are as

described above in the case of the unmodified plate for -OH groups and water molecules, respectively. The JUSTCORE optimization corresponds in this case to optimizing only these protons.

In case of more than one modification (e.g., two Al substitutions), the JUSTCORE optimization corresponds to the simultaneous optimization of all the relevant "core regions". The UPPERLEAFLET step consists of optimizing the 304 atoms above (in the z direction) an imaginary dividing line between the two "Ca rows" in the lower panel of Figure 1. By keeping the positions of the remaining 304 atoms (the "lower leaflet") constrained at their locations in the fully optimized, unmodified tobermorite plate one attempts to mimic the bulk structure of tobermorite.

6 Size convergence and electrostatic decoupling tests

The convergence of the results with respect to system size and the decoupling of the tobermorite plate with respect to its periodic replicas along the z direction (perpendicular to the plate) have been extensively investigated. The energy difference between an Al substitution in a BT and in a PT at the end of the JUSTCORE optimization (SIZE results in Supp. Table 1) was used as a reference. This energy difference was also calculated in a system twice as large as the original one in all three directions (2SIZE) and for a system 4 times as large (4SIZE). The former was constructed by having a 2x2 replica of the tobermorite plate where the "lower left corner" is a modified tobermorite plate with an Al in a BT or in a PT (in the configuration it has at the end of the JUSTCORE optimization) and the remaining 3 "parts" are unmodified tobermorite plates (the starting configuration for our JUSTCORE optimizations), so that one only has one Al atom in the system (note however that periodic boundary conditions are always used). A similar exercise is done for the 4SIZE system, see Supp. Figure 58. The 2SIZE systems then have x,y,z dimensions $(45.04, 58.24, 50.0)$ (in Å) and 2432 atoms and for the 4SIZE systems one has $(90.08, 116.48, 100.0)$ (Å) and 9728

	Δ E / Kcal/mol
SIZE	22.10
2SIZE	21.98
4SIZE	21.91
MT	22.46
WAVELET	22.90

Table 1: Energy differences between an Al substitution in a BT and a PT for different system sizes and using different methods to decouple electrostatic interactions in the z direction. See the text for further details.

atoms. The results in Supp. Table 1 show that indeed, despite the use of periodic boundary conditions in all three directions, the system size employed for all our calculations in this work together with the use of a neutralizing background are enough to essentially provide the energy difference between two "isolated" substitutions. As a further test, for the system with 608 atoms we have also performed single-point calculations for the PAIR-BRIDGE energy difference in a setup employing periodic boundary conditions in the x and y directions only, so that one has a real decoupling of the plate from periodic replicas along the z direction. Both with a Martyna-Tuckerman [1] (MT) and with a Wavelet [2, 3] based Poisson solvers, the results are essentially the same as with the setup used throughout this work, again justifying our approach. For completeness it should be mentioned that in these two cases the system size along z was of 50 Å, and not 25, due to the requirement that the unit cell be twice as large as the charge density for the MT solver. Merely due to the use of different computer facilities, all these tests employed CP2K version 2.2.218.

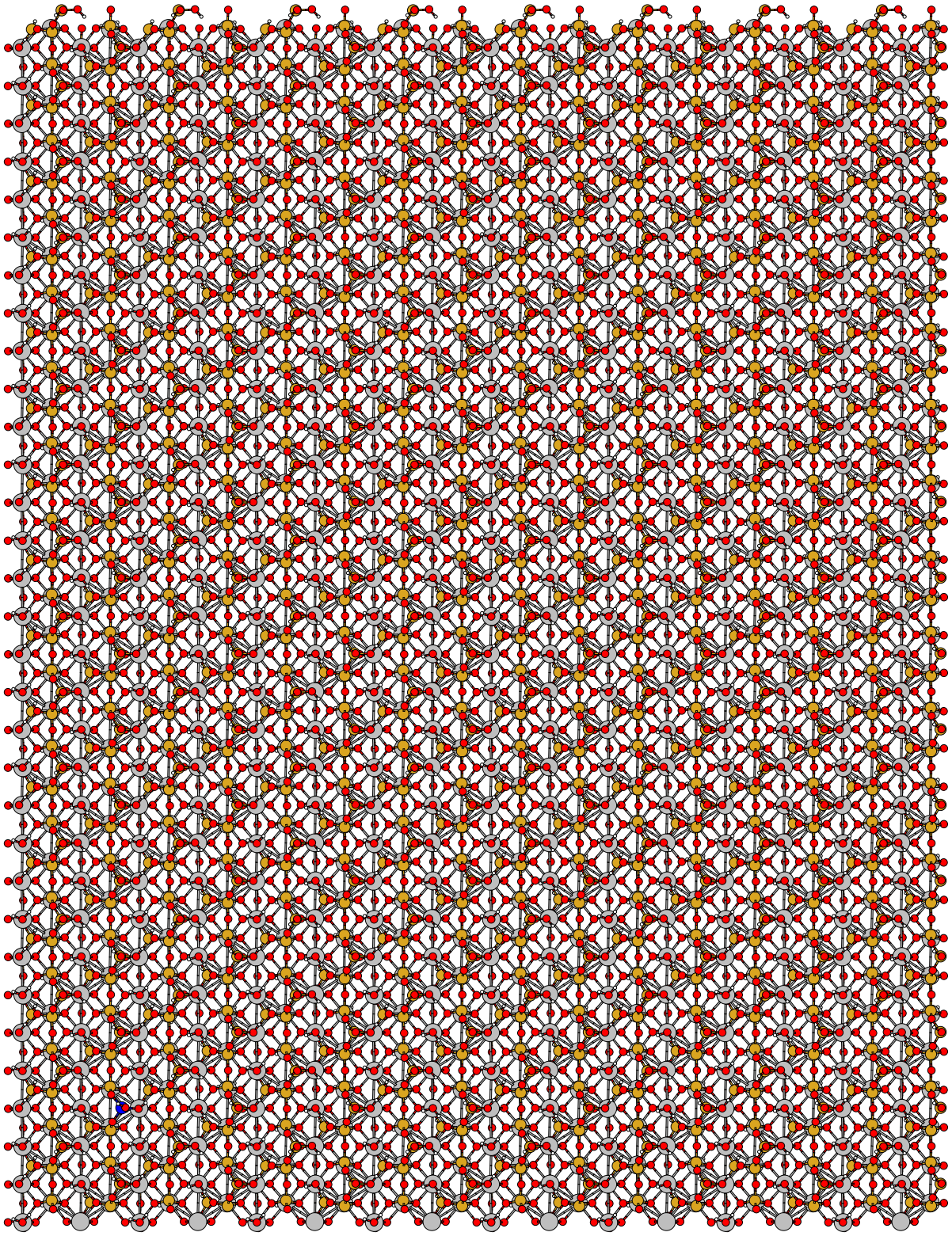

Supp. Figure 58: The 4SIZE system, used for size convergence tests, here with an Al substitution in a BT (blue in the lower left corner).

7 Data for Figures 3 and 4

System	Al-Al Dist.	Δ E	System	Al-Al Dist.	Δ E
$B_{2,5}B_{3,6}$	6.75	5.84	$B_{2,5}P_{4,7}$	11.74	23.40
$B_{2,5}B_{2,8}$	7.27	3.46	$B_{2,5}P_{2,10}$	12.78	19.51
$B_{2,5}B_{4,5}$	11.26	7.18	$P_{2,6}P_{2,7}$	3.15	54.92
$B_{2,5}B_{3,9}$	12.37	0.28	$P_{2,6}P_{2,4}$	4.11	48.02
$B_{2,5}B_{4,8}$	13.44	3.05	$P_{2,6}P_{3,5}$	5.76	46.77
$B_{2,5}B_{2,11}$	14.56	0.00	$P_{2,6}P_{3,7}$	6.66	44.61
$B_{2,5}P_{2,6}$	3.15	42.08	$P_{2,6}P_{3,4}$	6.70	44.44
$B_{2,5}P_{3,5}$	5.34	29.38	$P_{2,6}P_{2,9}$	7.26	44.79
$B_{2,5}P_{2,7}$	5.74	28.50	$P_{2,6}P_{3,8}$	8.85	41.91
$B_{2,5}P_{1,5}$	7.11	25.34	$P_{2,6}P_{3,2}$	9.65	40.79
$B_{2,5}P_{3,7}$	7.66	26.83	$P_{2,6}P_{2,10}$	10.49	41.62
$B_{2,5}P_{1,7}$	9.01	23.82	$P_{2,6}P_{4,6}$	11.26	42.99
$B_{2,5}P_{2,9}$	9.65	23.51	$P_{2,6}P_{2,1}$	11.39	40.25
$B_{2,5}P_{3,8}$	10.25	23.12	$P_{2,6}P_{4,7}$	11.73	42.32
$B_{2,5}P_{4,6}$	10.64	22.26	$P_{2,6}P_{2,12}$	14.56	36.88
$B_{2,5}P_{1,8}$	11.22	22.13			

Table 2: Data for Figure 3. Al-Al distances in Å and energy differences in Kcal/mol.

8 Calculation of Defect-Al distances for Figure 4

As can be appreciated in Supp. Figures 38 to 57, the defect was always created in the same location in all systems. Its position for the purpose of Defect-Al distance calculations was defined in all cases to be the average position of the two O atoms in the two silicate chain-terminating -OH groups, at the beginning of each geometry optimization. It is therefore a common, non-optimized location for all structures, but which represents sufficiently well for our purposes some average location of the defect even in the end of the UPPERLEAFLET optimizations (from which the coordinates of the Al atoms are taken). Since the coordinates of this "Defect position point" are the same in all cases then, we only provide the .xyz file for one of the structures represented above with it included, $D_{2,5}B_{2,8}$_WR.xyz (With Reference).

System	Def.-Al Dist.	Δ E	System	Def.-Al Dist.	Δ E
$D_{2,5}B_{1,6}$	6.00	0.00	$D_{2,5}P_{3,5}$	5.85	20.06
$D_{2,5}B_{2,8}$	7.31	4.23	$D_{2,5}P_{1,5}$	6.08	24.19
$D_{2,5}B_{3,6}$	7.52	0.20	$D_{2,5}P_{3,7}$	8.03	29.57
$D_{2,5}B_{1,9}$	11.95	10.02	$D_{2,5}P_{1,7}$	8.27	23.30
$D_{2,5}B_{4,5}$	12.16	5.03	$D_{2,5}P_{2,9}$	9.46	27.56
$D_{2,5}B_{3,9}$	12.77	8.23	$D_{2,5}P_{3,8}$	10.53	29.99
$D_{2,5}B_{4,8}$	14.16	4.85	$D_{2,5}P_{1,8}$	10.59	25.42
$D_{2,5}B_{2,11}$	14.56	2.21	$D_{2,5}P_{4,6}$	11.36	29.01
$D_{2,5}P_{2,6}$	2.53	22.54	$D_{2,5}P_{4,7}$	12.37	29.81
$D_{2,5}P_{2,7}$	5.40	25.03	$D_{2,5}P_{2,10}$	12.55	29.74

Table 3: Data for Figure 4. Defect-Al distances in Å and energy differences in Kcal/mol.

9 A few further notes on "error bars"

The generation of the different systems with two Al substitutions or one defect and one Al substitution exploited the symmetry of the upper leaflet of our base tobermorite plate. In particular, when considering the symmetry of the upper leaflet alone two adjacent pairing Si atoms are equivalent. The same is not true anymore, however, if one considers the lower leaflet also. To assess the possible influence of this, one performed a two-step geometry optimization for a system with a single pairing Al substitution in the position adjacent to the Al substitution in the PAIR system of Figure 2. Such a system (PAIR_NEWPOS, see Supplementary Figure 59) was more unstable than the PAIR one by 2.5 Kcal/mol.

As noted before our EOC and EOC_ref systems of Figure 2 are just the $D_{2,5}P_{2,6}$ and $D_{2,5}B_{2,8}$ also included in Figure 4, respectively, which in the latter were repeated for completion. From visual inspection of Figure 4 it can now be appreciated that the choice of a different DB system as reference for our EOC would mean that the corresponding energy difference in Table 1 could change by something of the order of ± 5 Kcal/mol. Note the correspondence between points in Figure 4 and structures given in the previous section.

A simple visual inspection of Supp. Figures 38 to 57 reveals that, for some systems where one defect is present, at the end of the UPPERLEAFLET optimization an H of one of the OH groups which terminate the silicate chain points in the direction of the O atom in the second

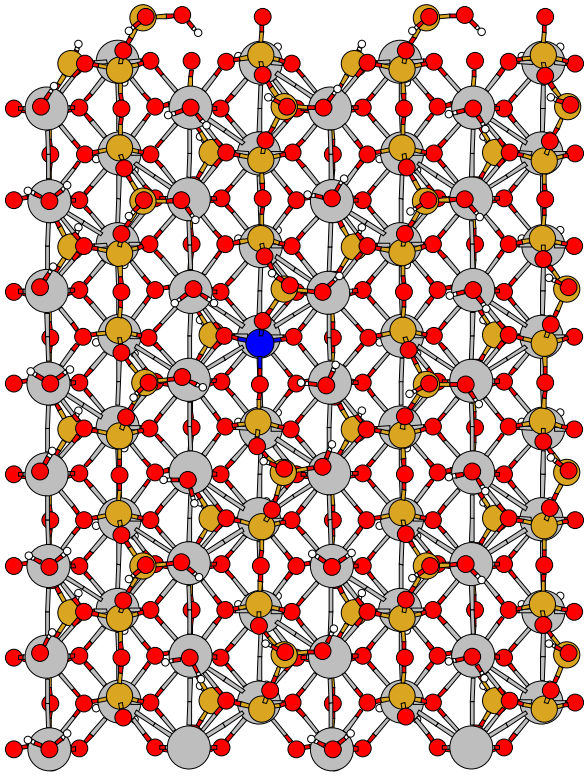

Supp. Figure 59: The PAIR_NEWPOS structure.

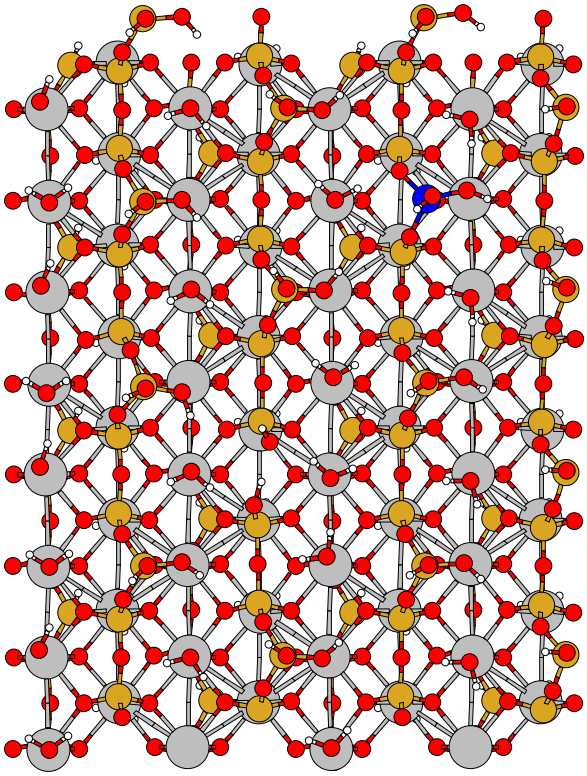

Supp. Figure 60: The $D_{2,5}B_{3,9-3,6}$ structure.

similar OH group. However, in other cases (namely the $D_{2,5}B_{3,9}$; $D_{2,5}B_{1,9}$; $D_{2,5}P_{2,9}$; $D_{2,5}P_{2,10}$; $D_{2,5}P_{3,7}$; $D_{2,5}P_{3,8}$; $D_{2,5}P_{4,6}$; and $D_{2,5}P_{4,7}$ systems) this does not happen. We will refer to this loosely as an "intra-defect H-bond", without any further analysis implied. As an example, the $D_{2,5}B_{3,6}$ system (intra-defect H-bond) is more stable than the $D_{2,5}B_{3,9}$ system (no intra-defect H-bond) by 8 Kcal/mol. We have performed a calculation were in the configuration of the last step of the UPPERLEAFLET optimization for the $D_{2,5}B_{3,6}$ system we shifted the Al atom to the position it has in the $D_{2,5}B_{3,9}$ system, and then reoptimized the structure at the UPPERLEAFLET level. This so-obtained "new" $D_{2,5}B_{3,9}$ system ($D_{2,5}B_{3,9-3,6}$, see the Supplementary Figure 60) had an energy differing from that of the $D_{2,5}B_{3,6}$ system by 0.7 Kcal/mol only.

In view of the previous paragraph, we also add that in the special case of the DIMER and DIMER_ref systems of Figure 2 the starting positions for the 4 H atoms which terminate silicate chains ("arround" the two defects) was not with all 4 "pointing up", as described in

general in sub-section "Details of the geometry optimization strategy". Rather, per defect one of them "pointed up" and the other pointed in the direction of the O in this first chain-terminating OH group (same x and z coordinates as the corresponding O atom, and y coordinate differing by 1 Å).

10 Effect of starting proton configurations for the DIMER systems

The orientation of the protons on the 4 chain-terminating OH groups in the cases containing a dimer with an Al substitution was found to have a sizeable influence on the energy of the system, and is therefore discussed here. All results are presented in Supp. Table 4 and molecular representations of the corresponding structures in Supp. Figures 62 to 66. As mentioned in the previous paragraph, for the DIMER systems in Figure 2 (see Supp. Figures 5 and 6 for molecular representations) we decided to have a starting configuration for the geometry optimizations with two "intra-defect H-bonds" enforced. With a dimer (two defects) there are four possibilities to realize this, depending on which OH groups donate and which accept H bonds, the latter having as starting configuration the proton "pointing up". The starting configuration for the DIMER system (DIMER_START) is presented in Supp. Figure 61. Both here and in Supp. Figure 5 the dimer is receiving (r) an H-bond from a nearby chain-terminating OH group, and donating (d; not to be confused with D used in our systematic notation for systems with one defect and one Al substitution) an H-bond. The same happens in the DIMER_ref system. In the DIMER system the dimer receives the (intra-defect) H-bond on an O atom coordinating to an Al, and this system will from now on be designated as PAIR_rd (see also the caption of Supp. Table 4). When for DIMER_ref (henceforth BRIDGE_rd) we change the starting configuration so that the dimer donates two H-bonds (BRIDGE_dd system), this is not very consequential for the energy in the end of the UPPERLEAFLET optimization. This is however not the case for PAIR_rd, the

PAIR_dd system being more unstable by 12.4 Kcal/mol. The orientation of the intra-defect H-bond which does not involve O's coordinating to the Al atom also does not seem to be very important (PAIR_rr system). One therefore concludes that the difference in energy between the PAIR_rd/PAIR_rr and PAIR_dd systems is the fact that in the former two an O atom coordinating to the Al accepts, rather than donates, an H-bond (the length of the accepted H-bonds is 1.44 Å in both cases). This was further tested by studying a $D_{2,5}P_{2,6}$ system (see Supp. Figure 46) where in the starting configuration one of the chain-terminating H atoms was "pointing up" but the other (on the O which also coordinates to the Al atom) pointed in the direction of the opposing chain-terminating O atom (which coordinates to the H atom "pointing up") (see Supp. Figure 66). This $D_{2,5}P_{2,6}$_d system, where loosely speaking the Al donates, rather than accepts an H-bond, is more unstable than the corresponding $D_{2,5}P_{2,6}$ by 17.2 Kcal/mol (in the end of the UPPERLEAFLET optimization; for $D_{2,5}P_{2,6}$ the length of the accepted H-bond is 1.54 Å). This therefore shows the big propensity of the Al to receive an H-bond, be it in a dimer or merely in the end of a chain. A similar exercise was performed for the $D_{2,5}P_{2,7}$ system, by having a starting structure with the side of the dreierketten chain where the Al is closest to the defect accepting, rather than donating an H-bond (the opposite of what is displayed in Supp. Figure 47; structure not shown). In the end of the UPPERLEAFLET optimization, this was more stable than $D_{2,5}P_{2,7}$ by merely 4.8 Kcal/mol. For completeness, in the case of PAIR systems we have also studied the remaining possibility of having the dimer receiving one and donating one H-bond (PAIR_dr). Even though in this case the Al is not receiving an H-bond from the chain-terminating OH group facing it, the energy is almost the same as for the PAIR_rd system. It will not be our goal to definitively explain the extra stability of PAIR_dr with respect to PAIR_dd, but we still mention two noticeable differences between the two systems: in PAIR_dd the O on the Al-O-H group accepts a strong H-bond from a neighbouring water molecule (1.63 Å); in PAIR_dr the same O atom accepts two H-bonds from neighbouring water molecules (1.62 and 1.96 Å). Besides this, the length of the donated H-bond by the Al-O-H group is 1.82 Å for PAIR_dd but 1.64

Å for PAIR_dr.

	Δ E / Kcal/mol
DIMER_ref (BRIDGE_rd)	0.0
DIMER (PAIR_rd)	23.0
BRIDGE_dd	-3.2
PAIR_dd	35.4
PAIR_rr	18.9
PAIR_dr	23.4

Table 4: Relative energies for systems with a dimer and one Al substitution which differ between themselves in the location of the Al and/or the orientation of the H-bonds from/to the two O atoms which terminate the dimer ("intra-defect H-bonds", as already used before, again without any analysis implied other than the visual inspection of the systems in Supp. Figures 5, 6 and 62 to 65). BRIDGE refers to systems with an Al substitution in the same BT as in the DIMER_ref system of Supp. Figure 6, and PAIR to systems with an Al in the same PT as in the DIMER system. "r" stands for receiving and "d" for donating, and indicates whether the two O atoms which terminate the dimer are receiving or donating H-bonds from/to the other chain-terminating O atoms facing them. The first letter stands for the O atom coordinating to the Al in the PAIR systems. All energies are relative to that of the DIMER_ref system (BRIDGE_rd in the new nomenclature).

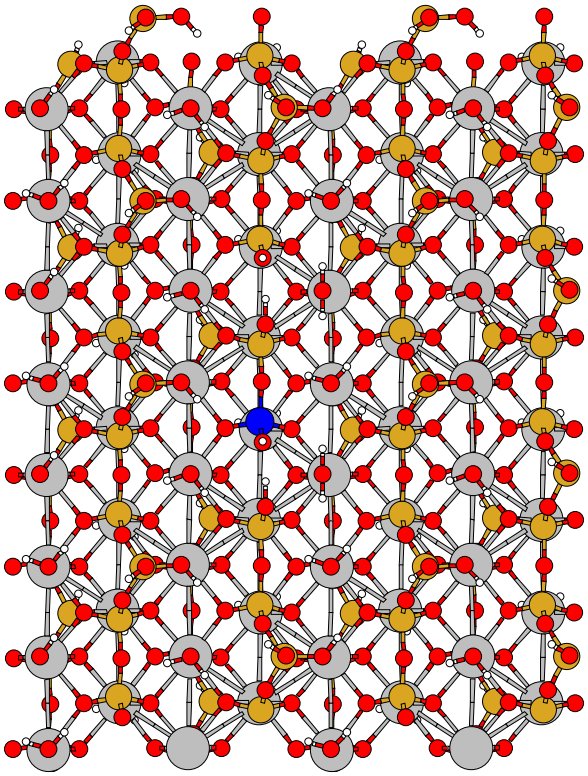

Supp. Figure 61: DIMER_START: starting configuration for the JUSTCORE geometry optimization of the DIMER (PAIR_rd) system in Supp. Figure 5. The starting configurations for the DIMER_ref, BRIDGE_dd, PAIR_dd, PAIR_rr and PAIR_dr systems all have two "intra-defect H-bonds" enforced from the beginning like here (and also similarly with the remaining 2 of the 4 chain terminating protons "pointing up"), but differ depending on if these are donated (d) or received (r) by the dimer. As can be appreciated below, the situation enforced from the beginning is by large maintained in the end of the UPPERLEAFLET optimization, for each case.

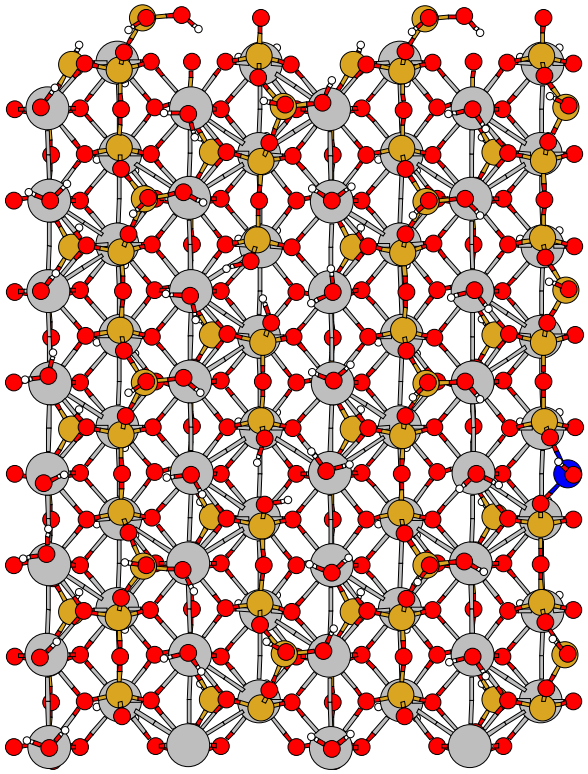

Supp. Figure 62: The BRIDGE_dd structure.

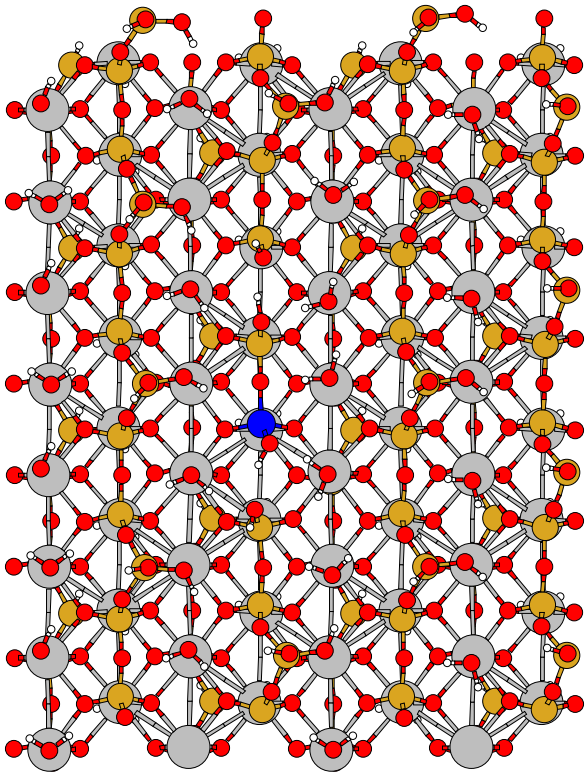

Supp. Figure 63: The PAIR_dd structure.

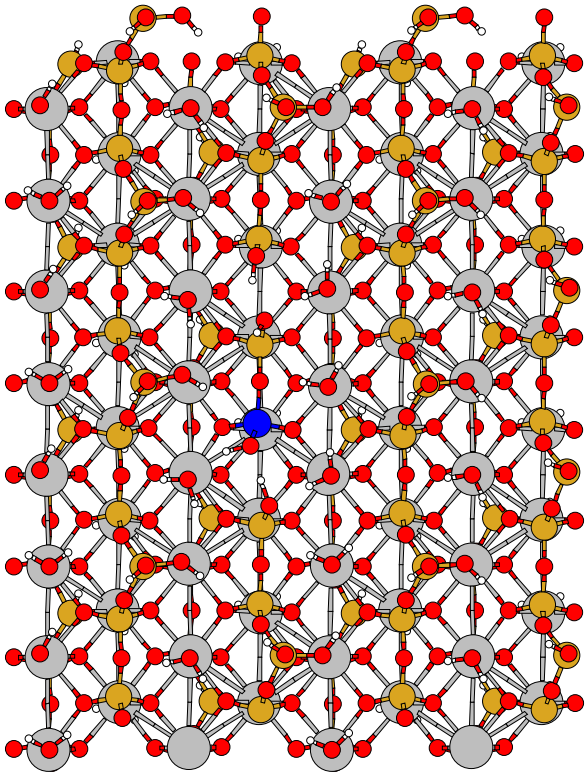

Supp. Figure 64: The PAIR_rr structure.

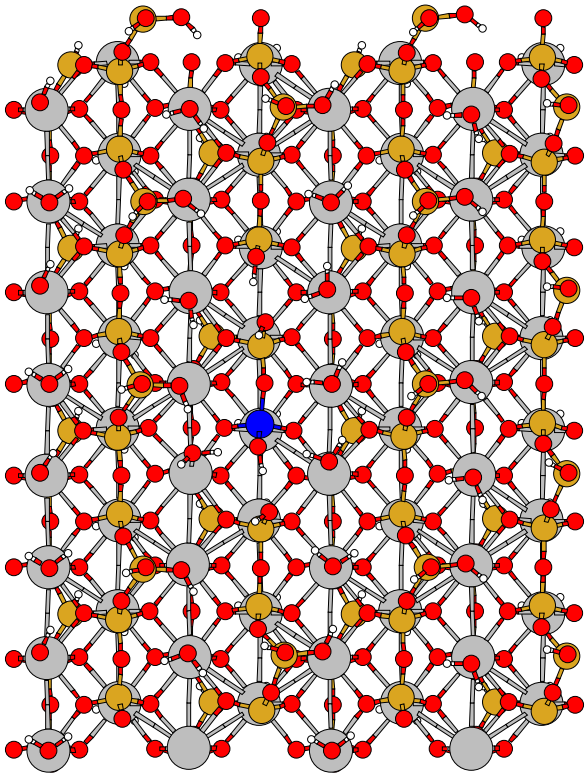

Supp. Figure 65: The PAIR_dr structure.

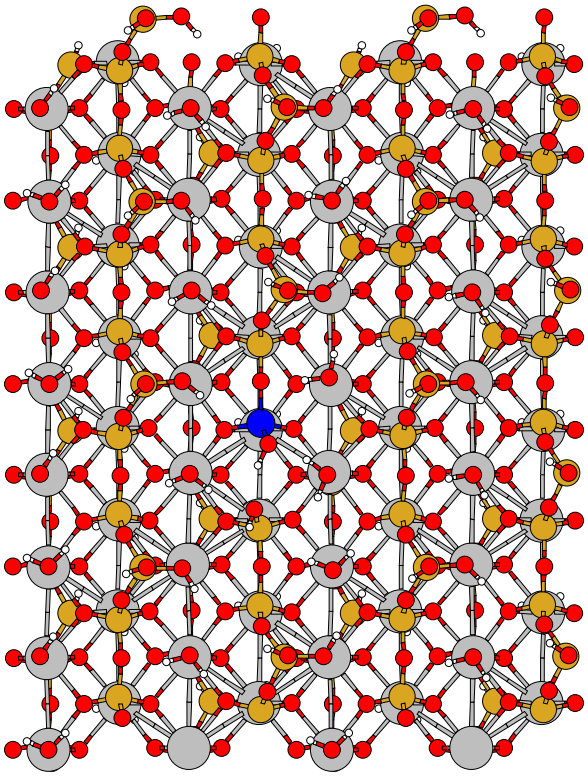

Supp. Figure 66: The $D_{2,5}P_{2,6}$_d structure.

References

[1] G. J. Martyna and M. E. Tuckerman, J. Chem. Phys. **110**, 2810 (1999).

[2] L. Genovese, T. Deutsch, A. Neelov, S. Goedecker, and G. Beylkin, J. Chem. Phys. **125**, 074105 (2006).

[3] L. Genovese, T. Deutsch, and S. Goedecker, J. Chem. Phys. **127**, 054704 (2007).